RECENT ADVANCES IN HEAT TRANSFER RESEARCH AND MODELLING

Henryk Anglart, Professor
Director of the Center for Nuclear Technology
AlbaNova University Center
KTH Royal Institute of Technology

www.reactor.sci.kth.se

Outline

- Introduction
- Thermal mixing leading to thermal fatigue
- Towards DNB
- Annular two-phase flow modeling
- Towards dryout
- Post-dryout heat transfer
- Conclusions

Introduction – Thermal Mixing and Fatigue

- Thermal fatigue is one of the main ageing mechanisms considered in evaluation of the reduction of the lifetime of plant components
- It is highly relevant to components where mixing of two non-isothermal streams occurs
- A thermal fatigue related event occurred in Forsmark and Oskarshamn NPPs in 2008.
- In both cases several control rod extenders were completely broken and some had incipient cracks

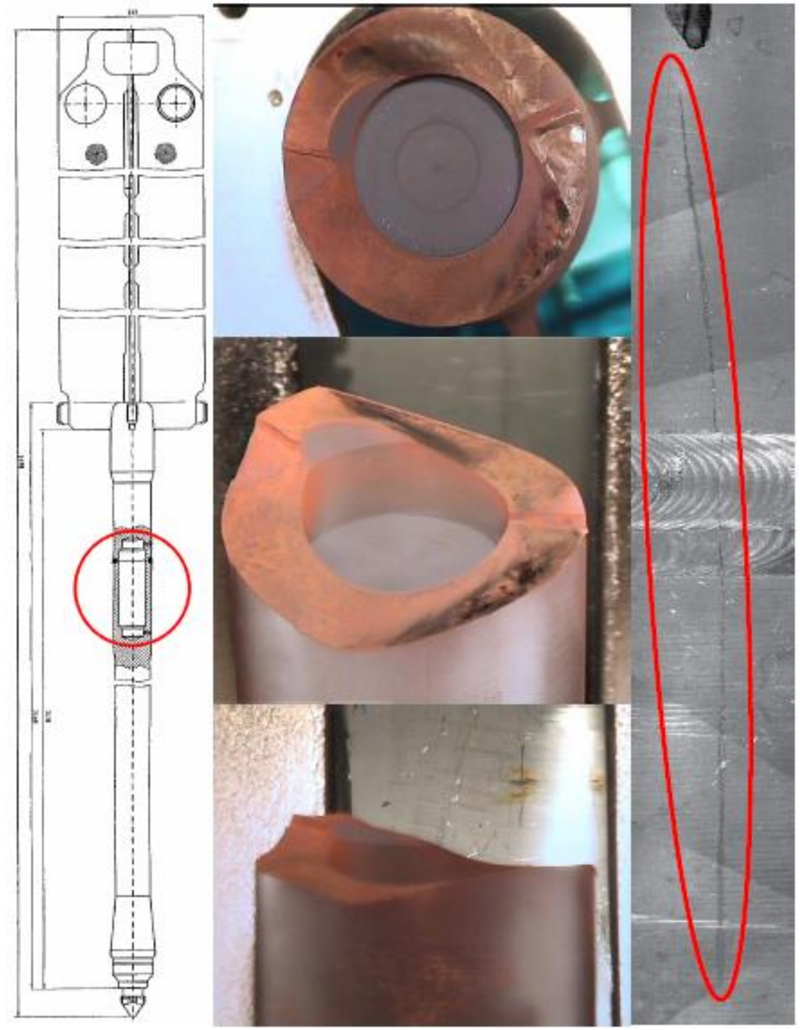

Tinoco et al. ICONE18, 2010

Background

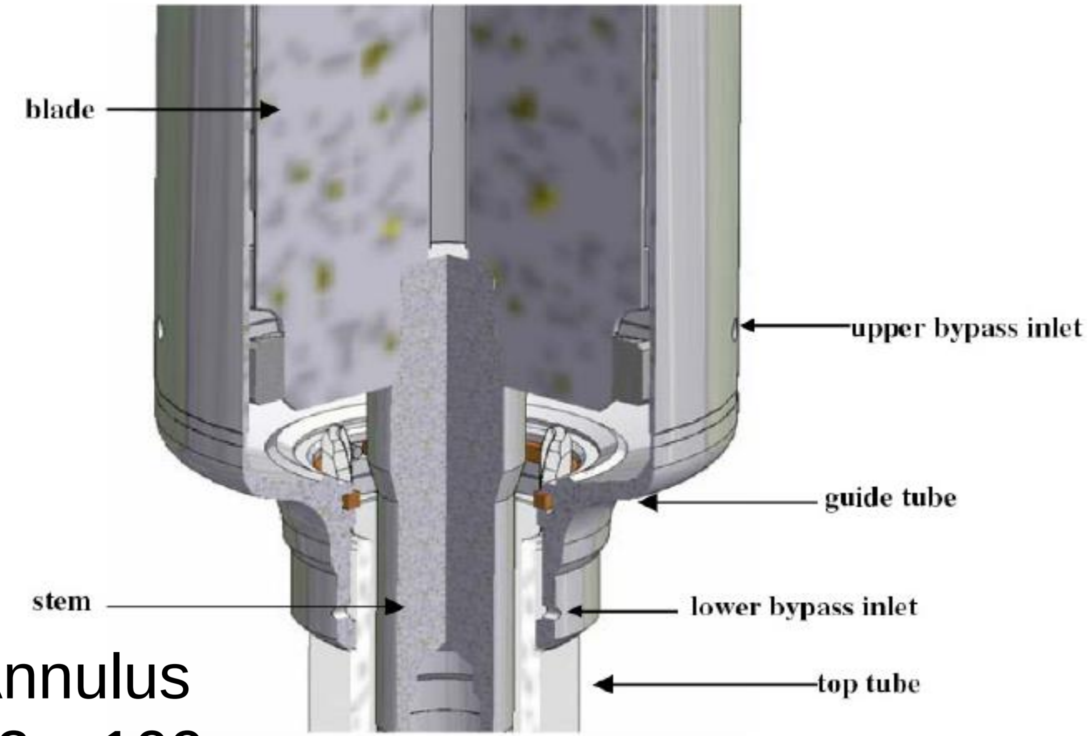

Annulus
92 x 109 mm

hot inlet: 4 x Ø8 mm
2.12 kg/s

Details of control rod housing and bypass flow in BWR (Tinoco, ICONE18)

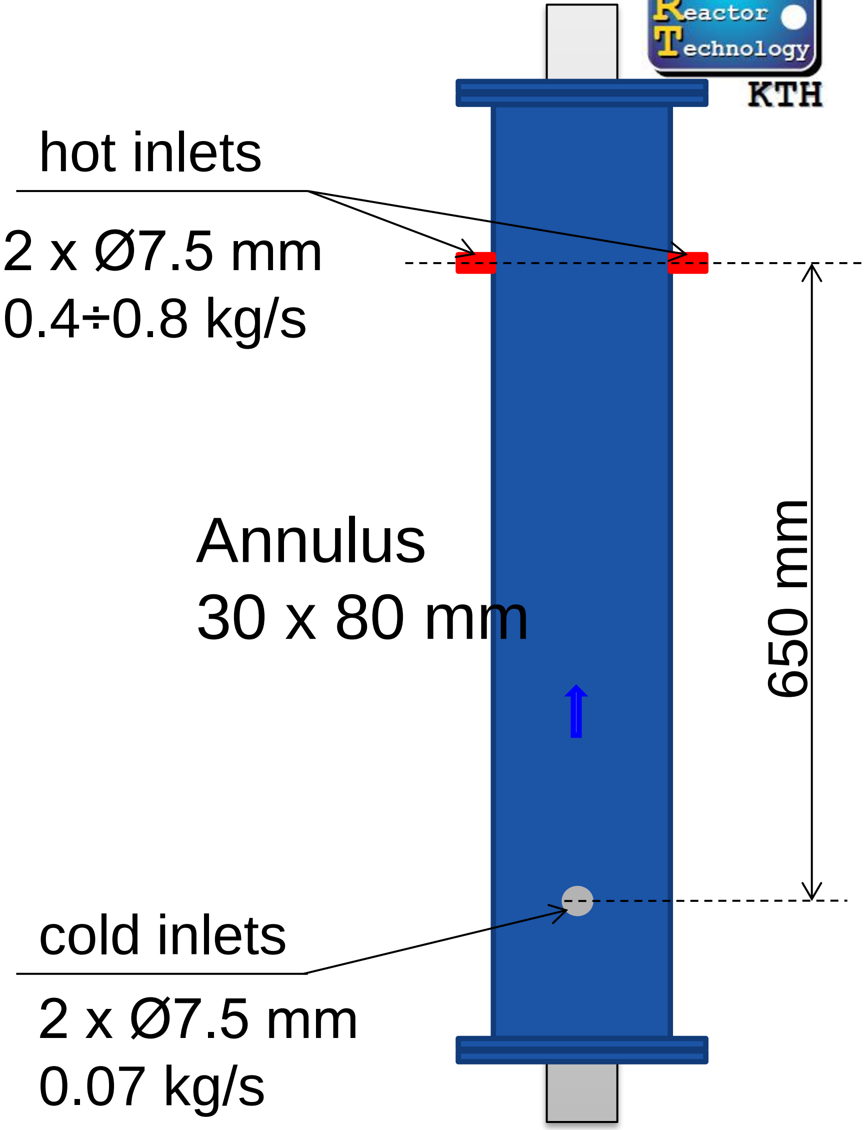

Schematic of test section used in experiments

Experimental Facility

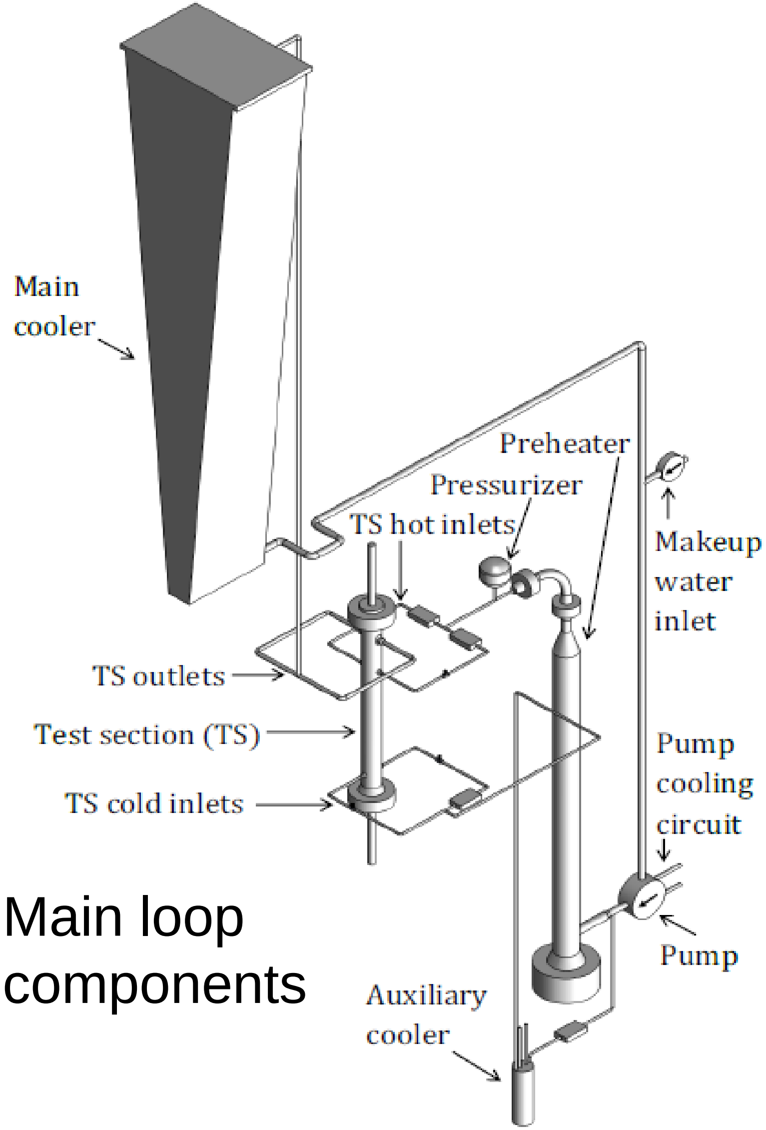

Main loop components

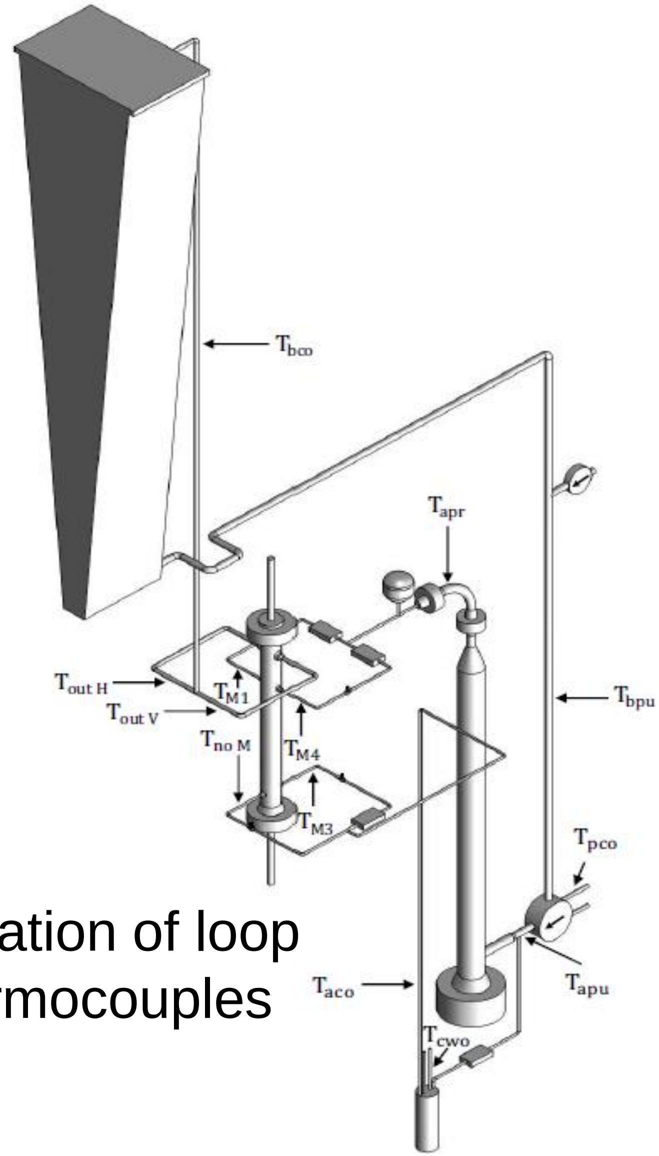

Location of loop thermocouples

Outer Tube of Test Section

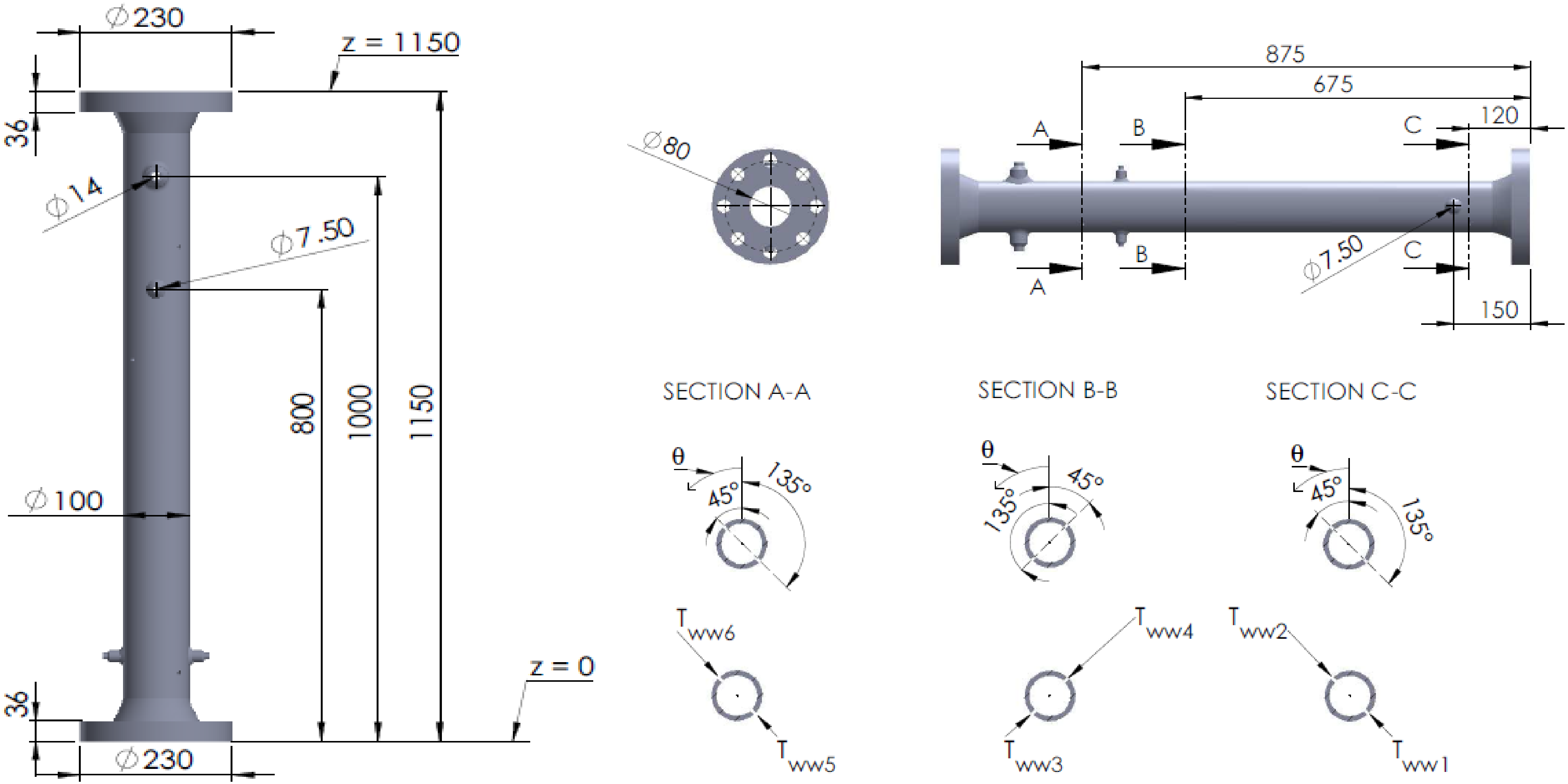

Inner Tube of Test Section

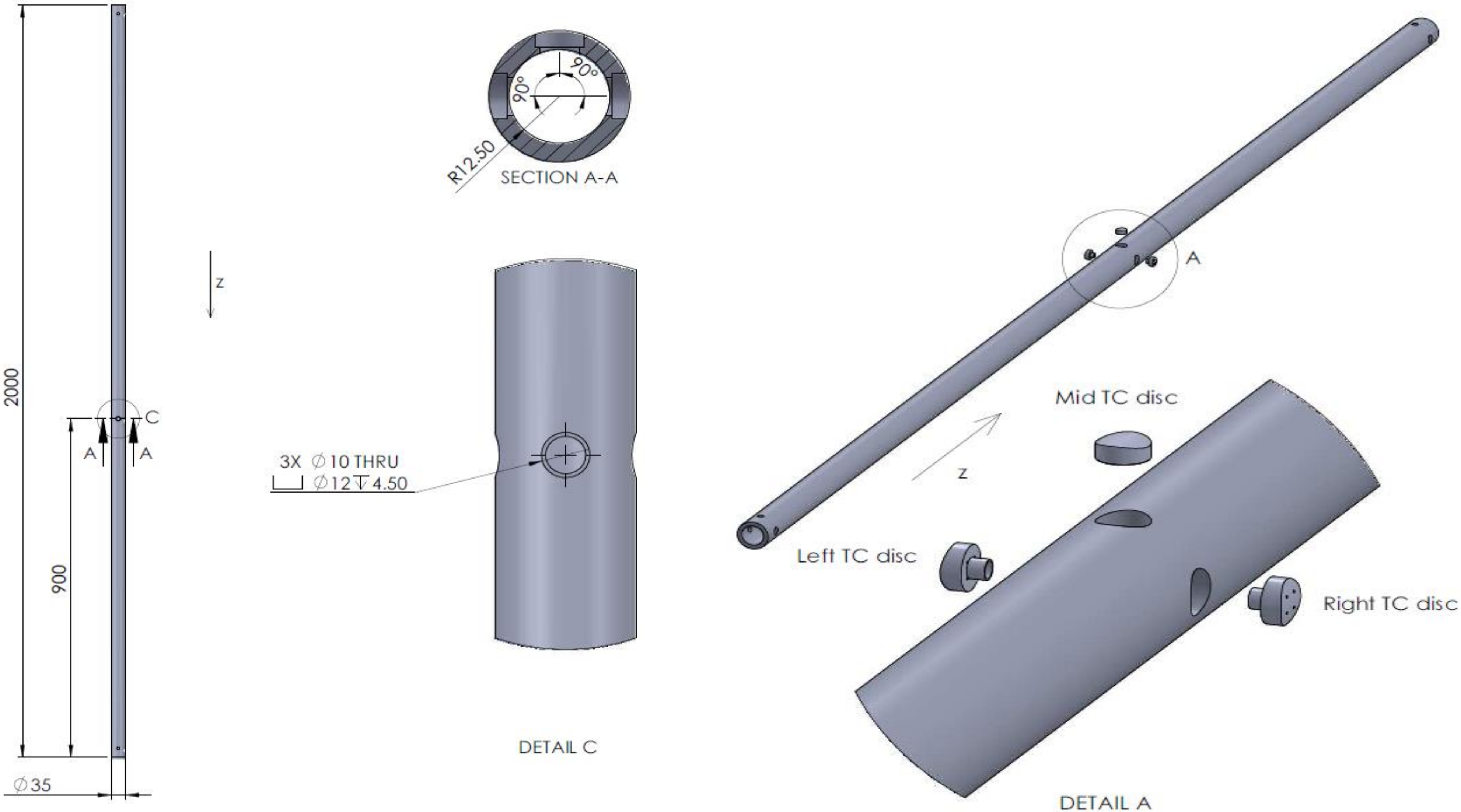

Thermocouple Discs

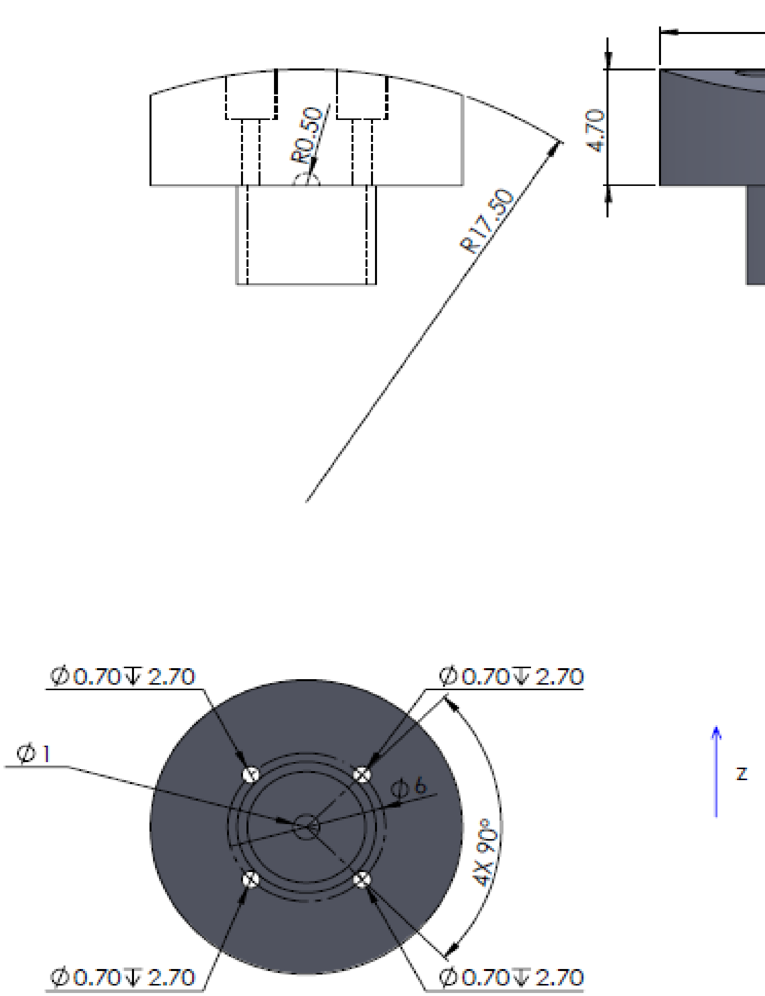

Left and right TC discs

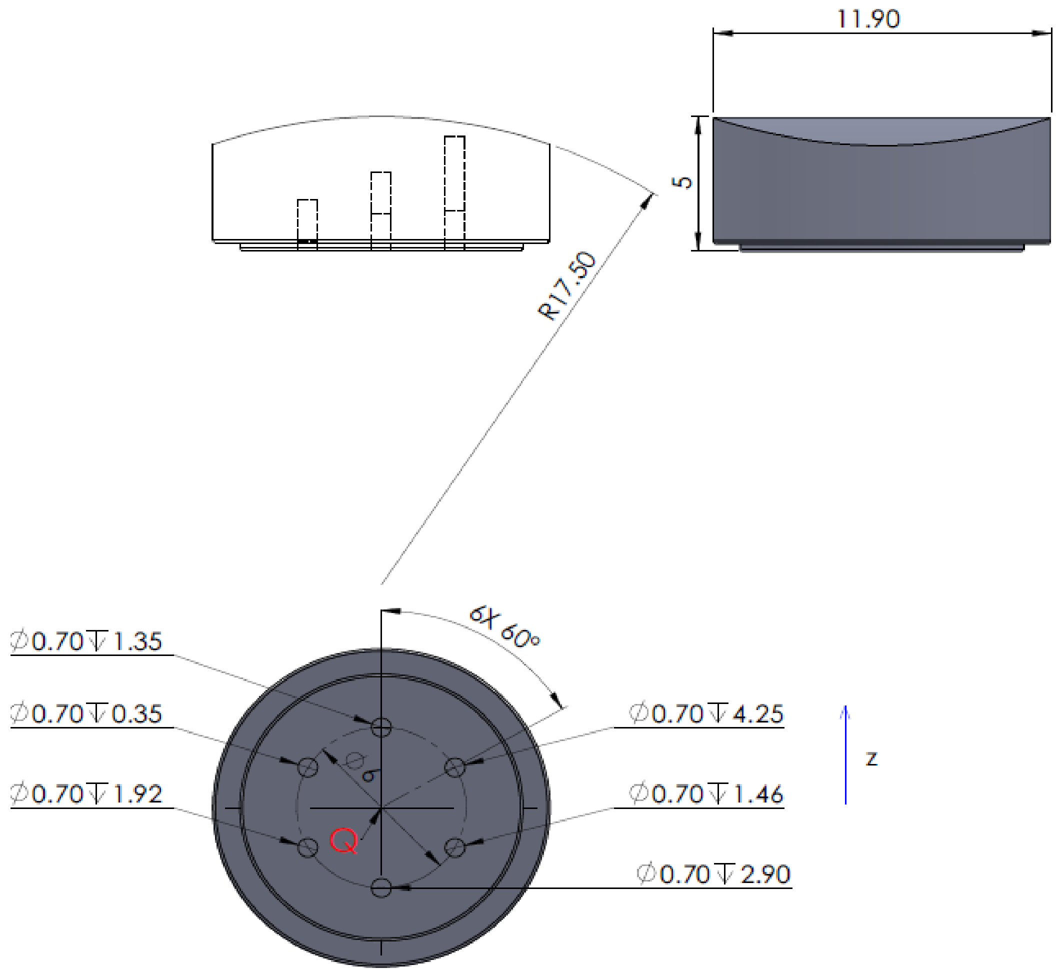

Central TC disc

Thermocouple Mounting in Disc

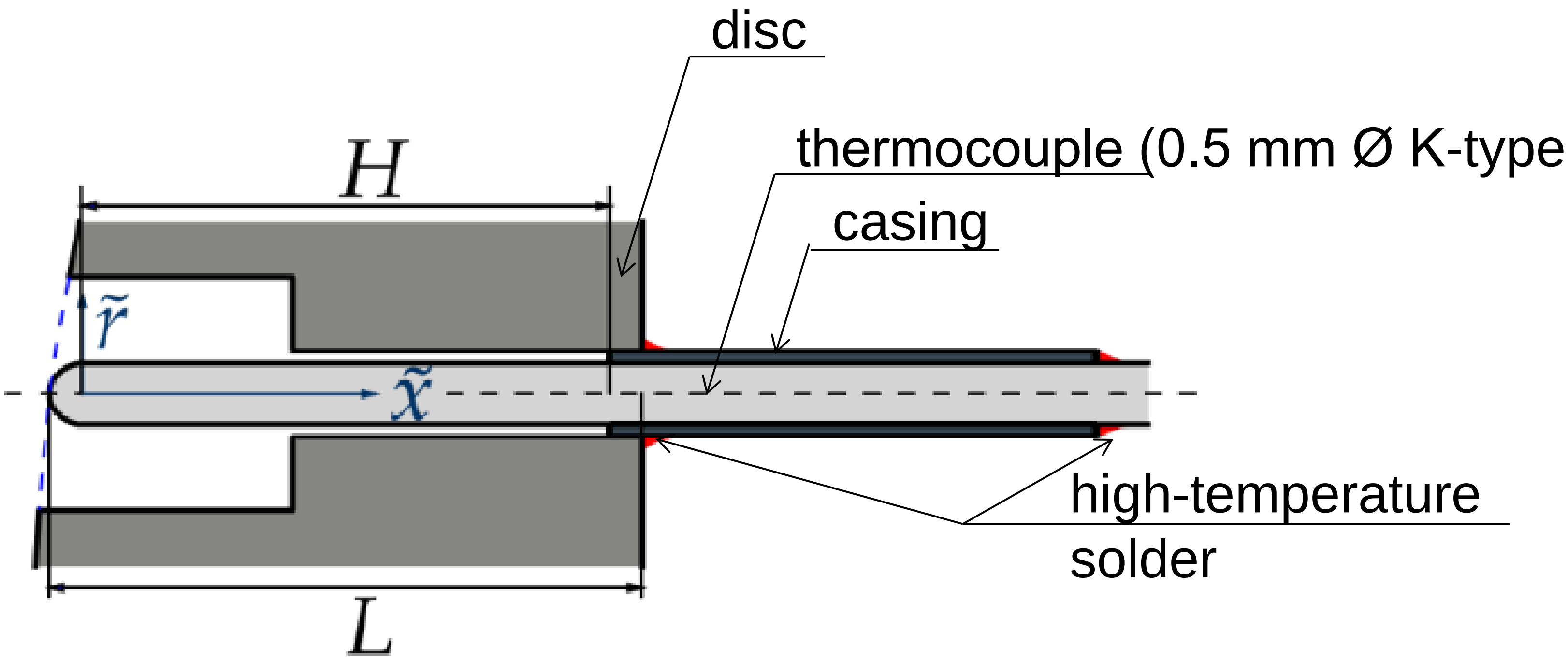

Direct water temperature measuring thermocouple used in left and right discs (Bergagio et al., NURETH-16, 2015)

Experimental Matrix

Case	Cold inl. flow (kg/s)	Cold inl. temp. (K)	Hot inl. flow (kg/s)	Hot inl. temp. (K)
1	0.07	333.15	0.8	549.15
6	0.07	423.15	0.6	549.15
9	0.07	333.15	0.4	549.15

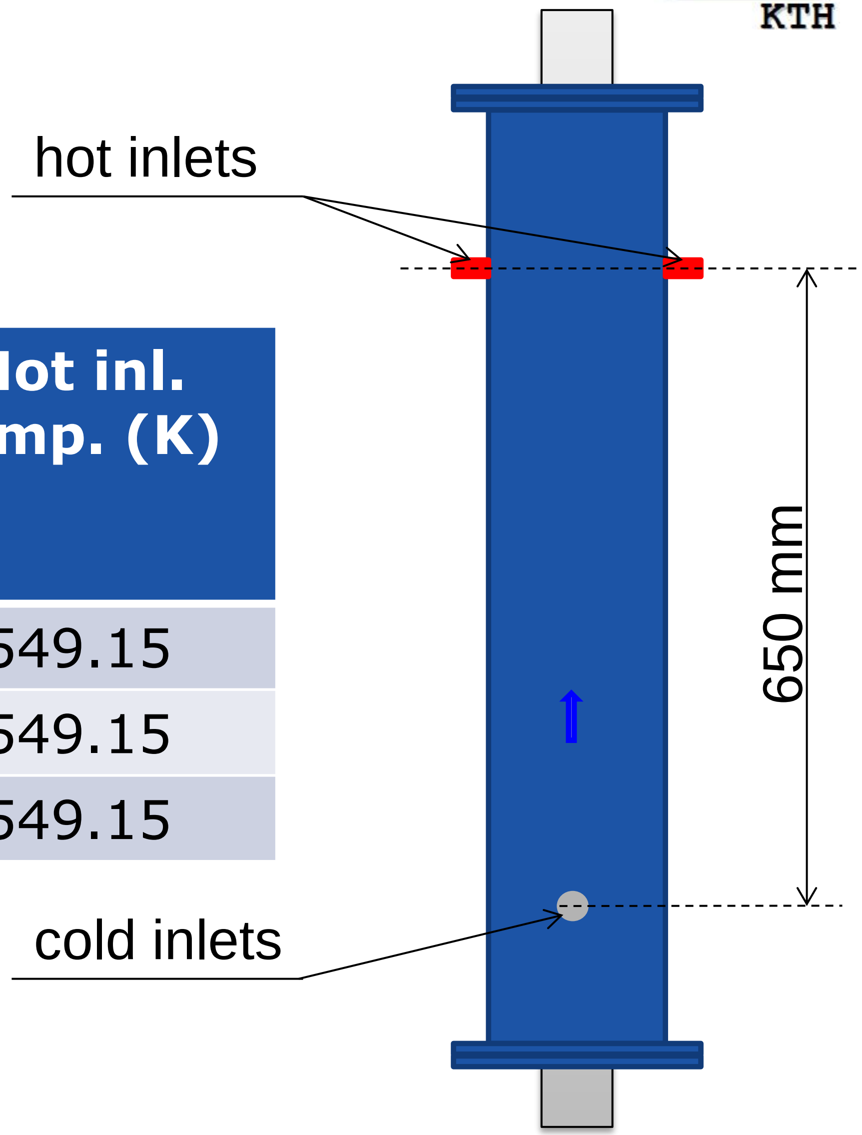

Measured Wall Temperature

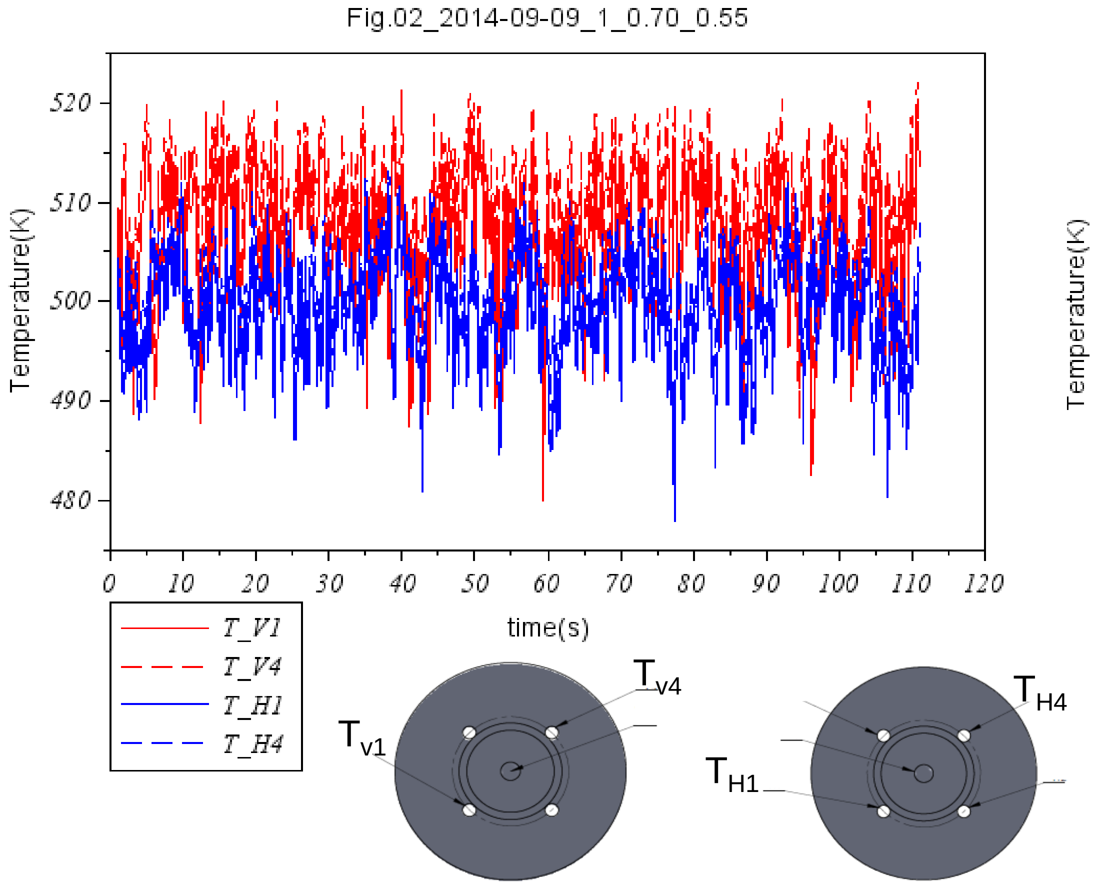

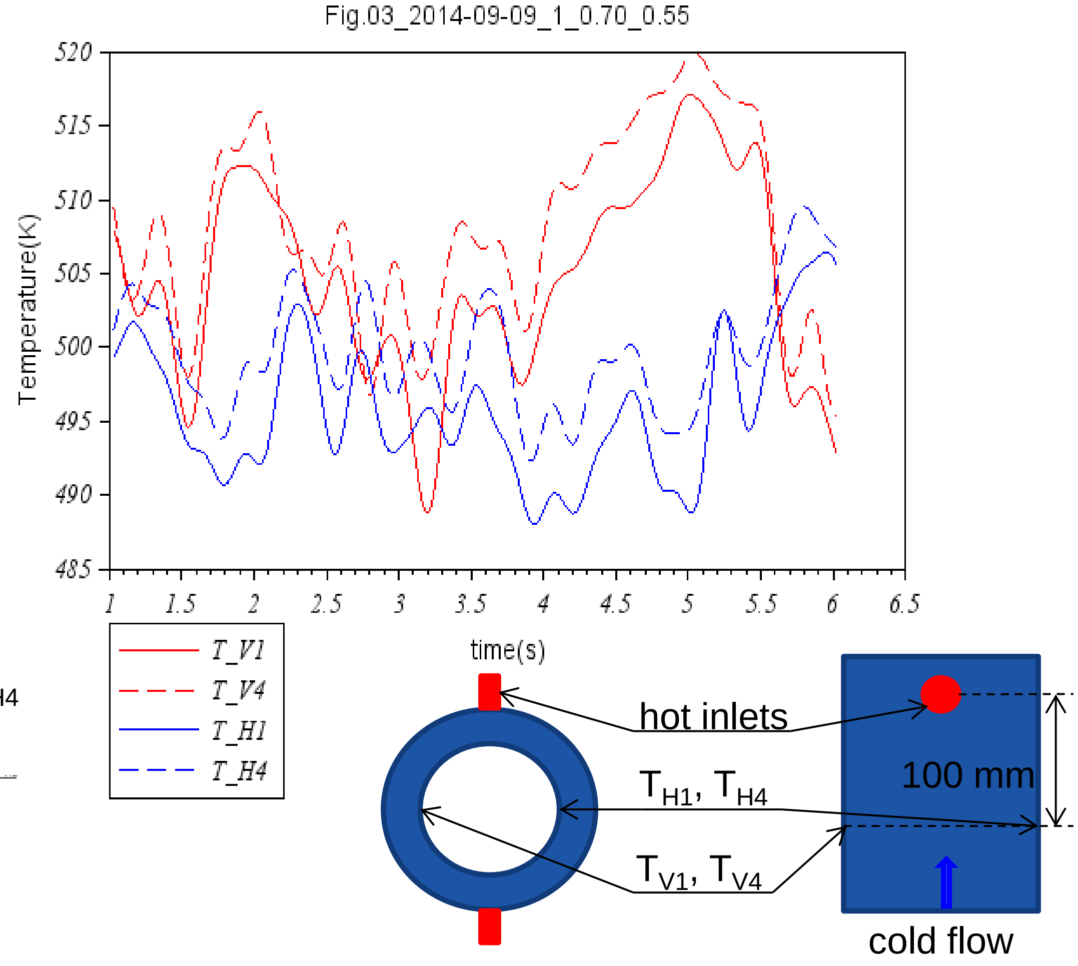

Case 1, axial location 0.7 m, angle 0.55° (T_{cold} = 60 °C, W_{hot} = 0.8 kg/s)

Measured Wall Temperature

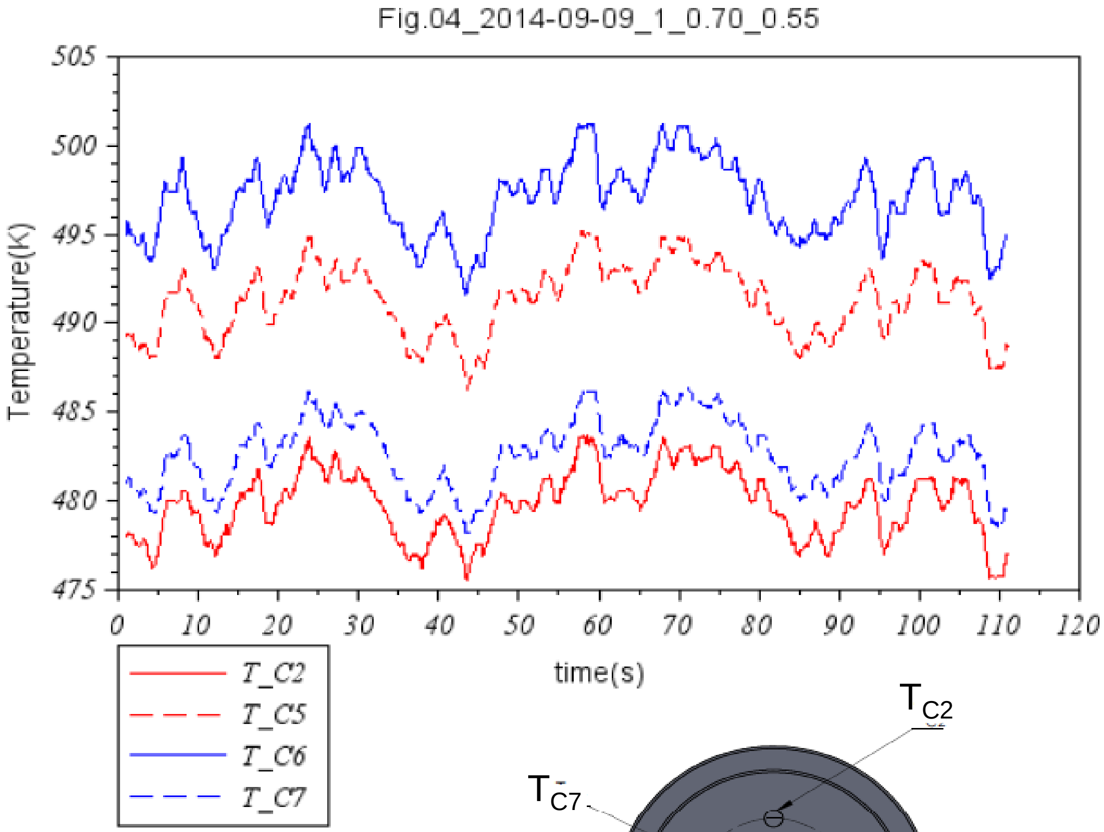

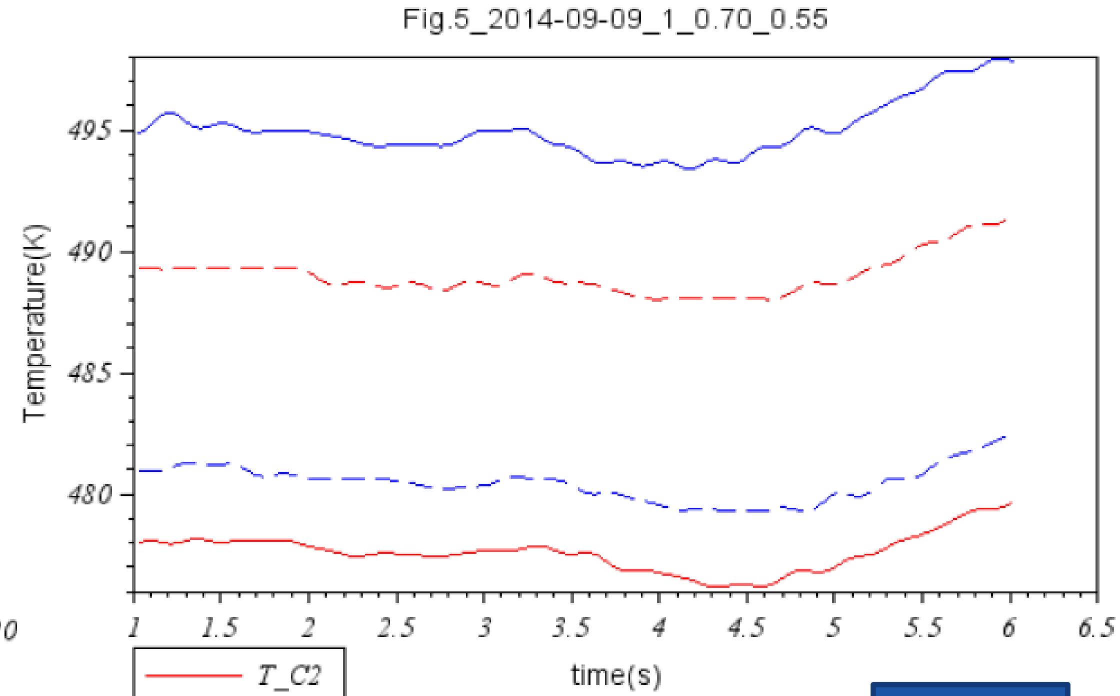

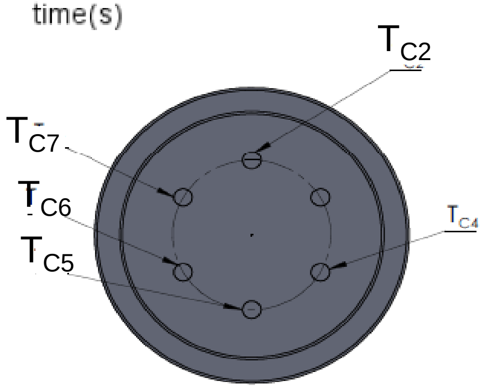

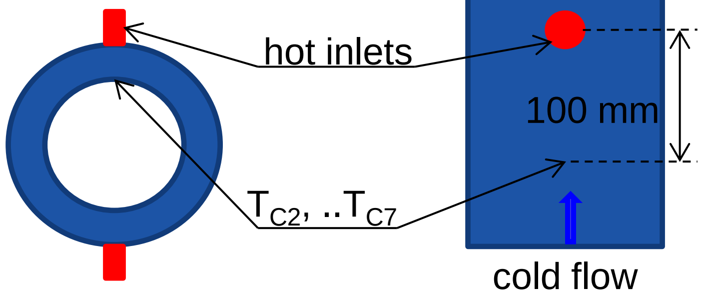

Case 1, axial location 0.7 m, angle 0.55° (T_{cold} = 60 °C, W_{hot} = 0.8 kg/s)

Measured Wall Temperature

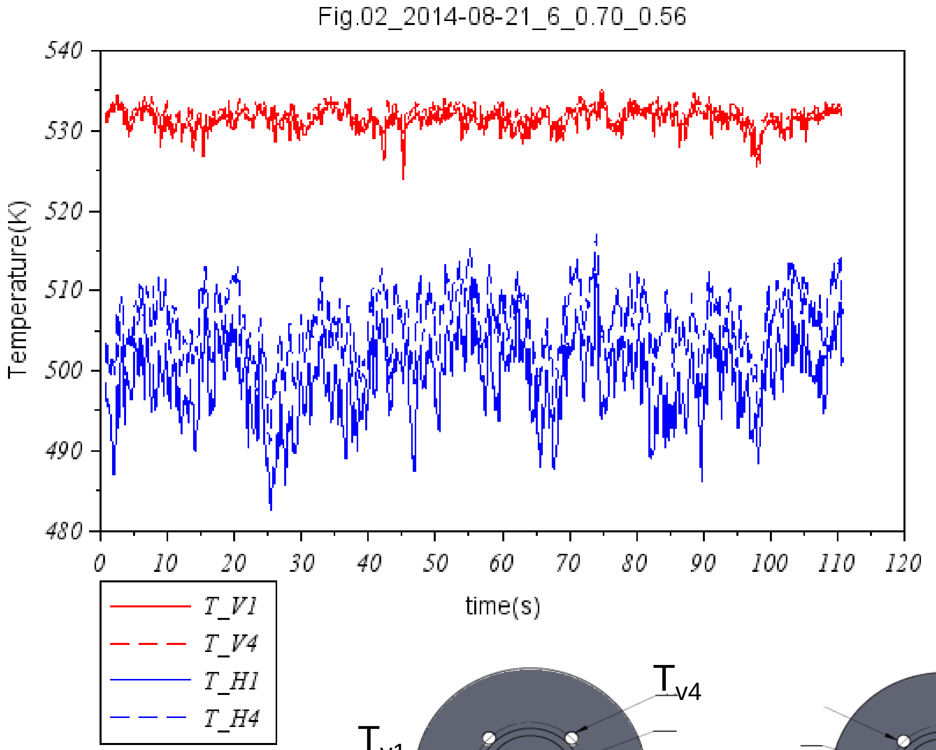

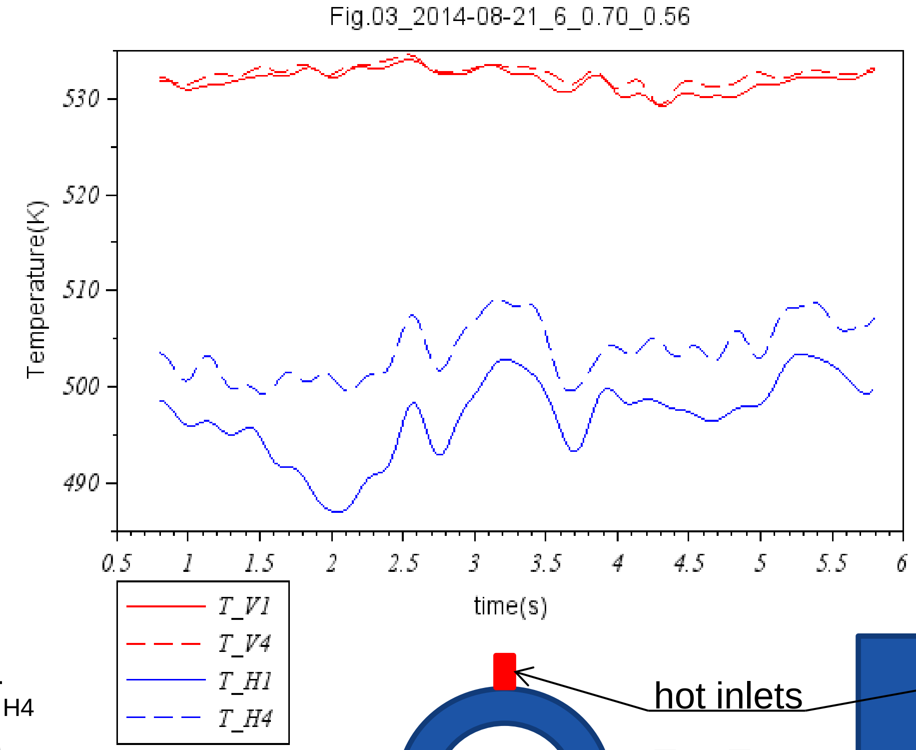

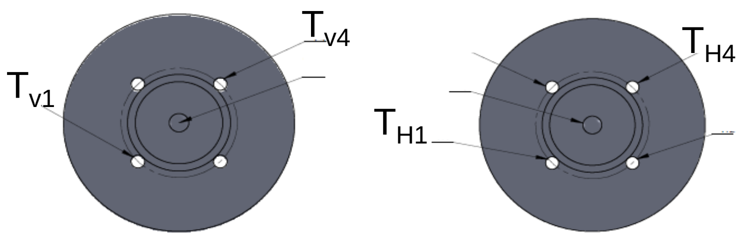

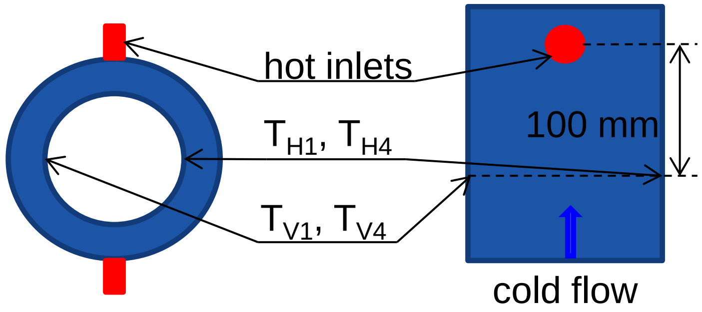

Case 6, axial location 0.7 m, angle 0.56° (T_{cold} = 150 °C, W_{hot} = 0.6 kg/s)

Measured Wall Temperature

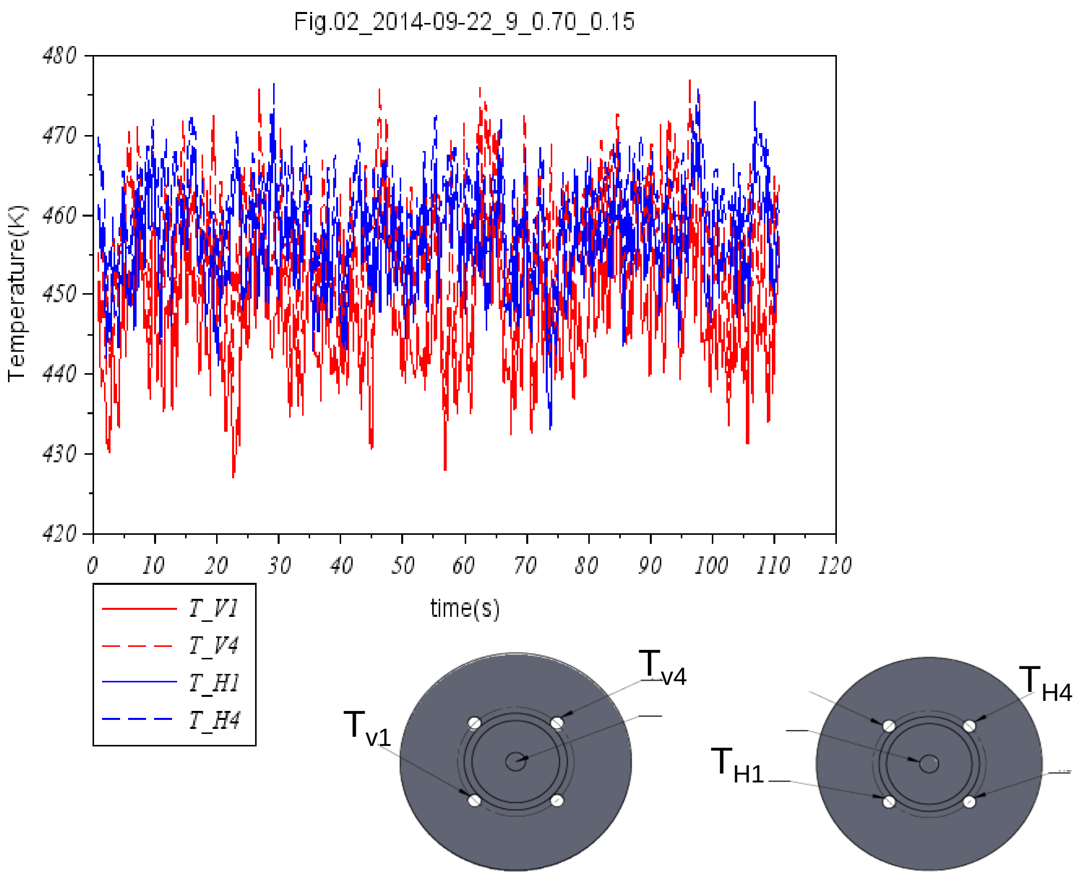

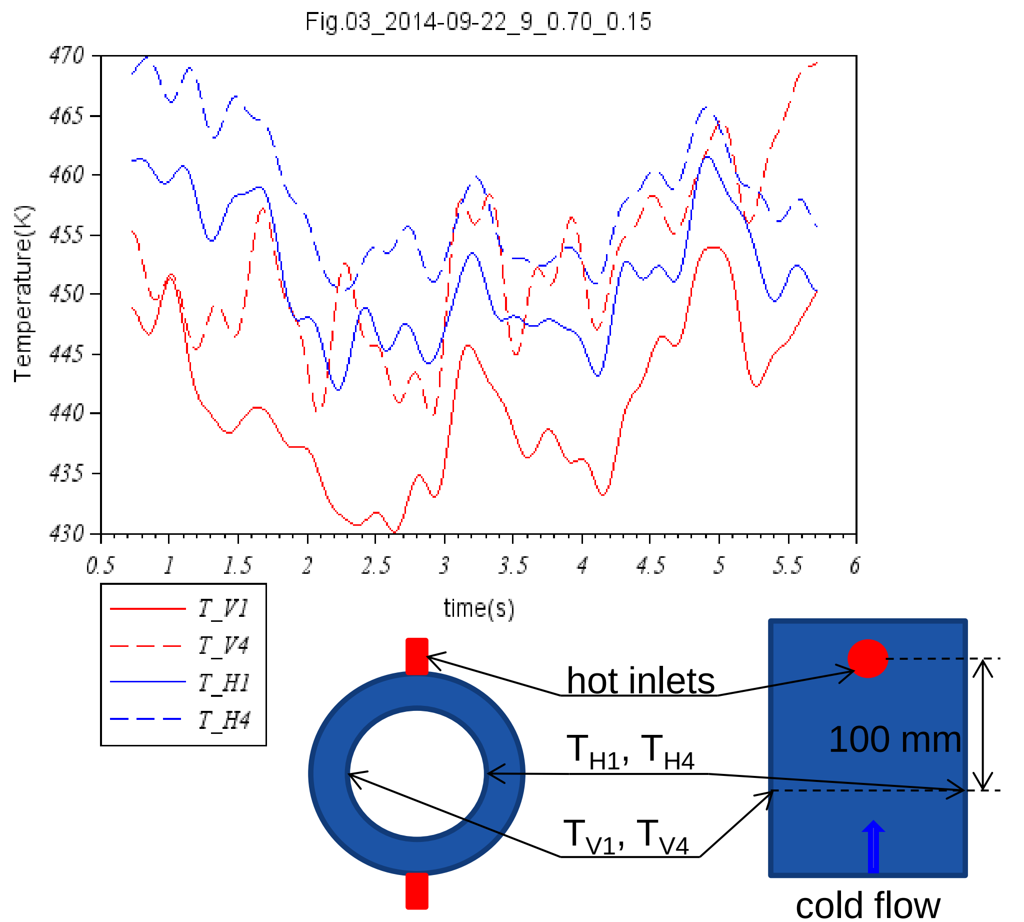

Case 9, axial location 0.7 m, angle 0.15° (T_{cold} = 60 °C, W_{hot} = 0.4 kg/s)

LES prediction of thermal mixing

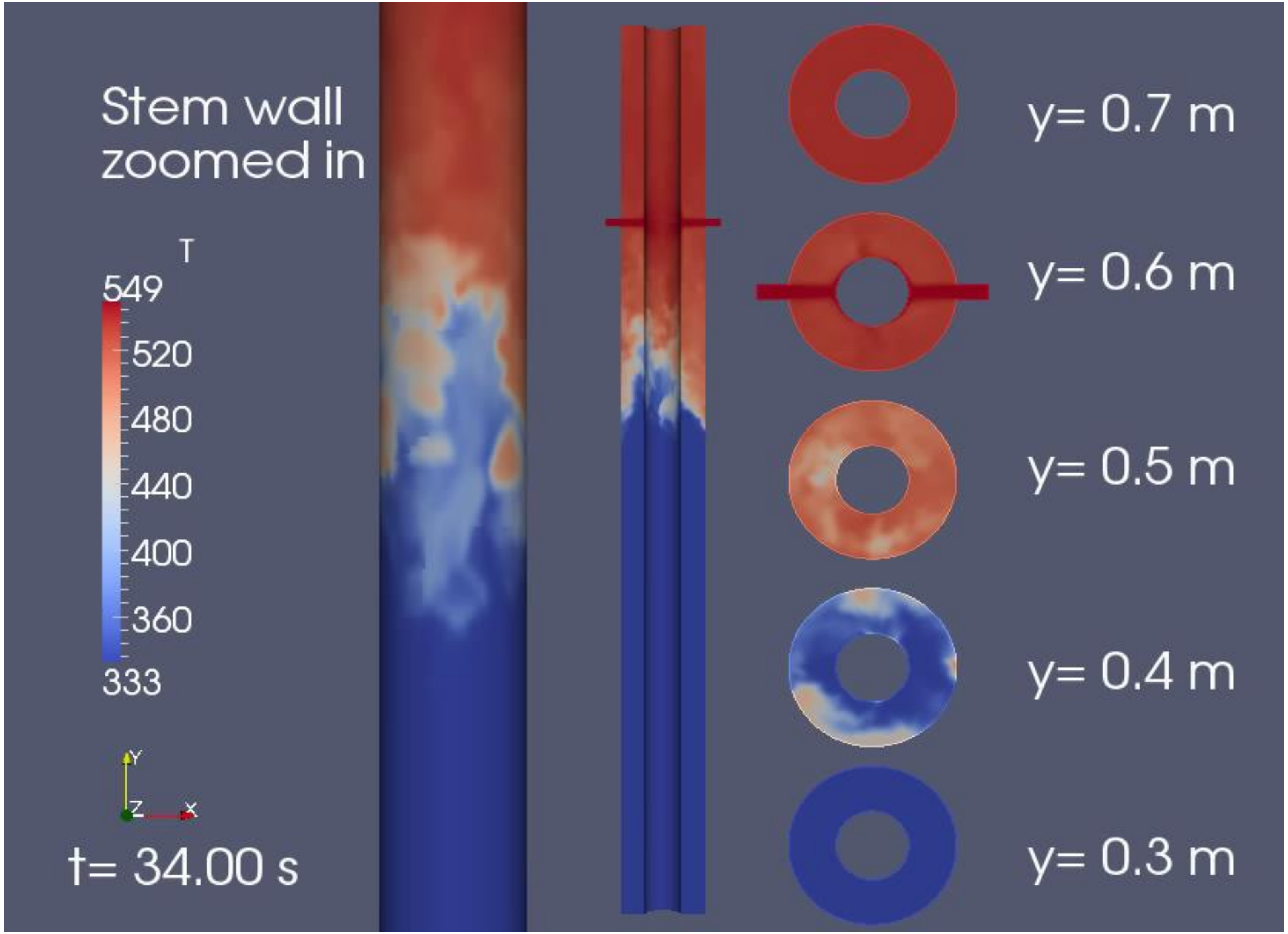

Reijo Pegonen

ROYAL INSTITUTE OF TECHNOLOGY

Boiling Heat Transfer

- Prediction of CHF in LWR fuel assemblies still remains in the focus of TH research
- The main difficulties in prediction of DNB stem from
  - Multiphysics problem with a large span of length scales
    - surface features [nm]
    - liquid microlayers beneath bubbles [μm]
    - bubbles [mm]
    - bulk flow features [cm]
- The main difficulties in prediction of dryout stem from
  - high voids requiring modelling of flow pattern transition
  - resolving thin liquid film [μm]
  - prediction/modelling of the drop size distribution
  - modelling of the entrainment rates
  - liquid film stability and breakup

Boiling regimes with constant wall heat flux

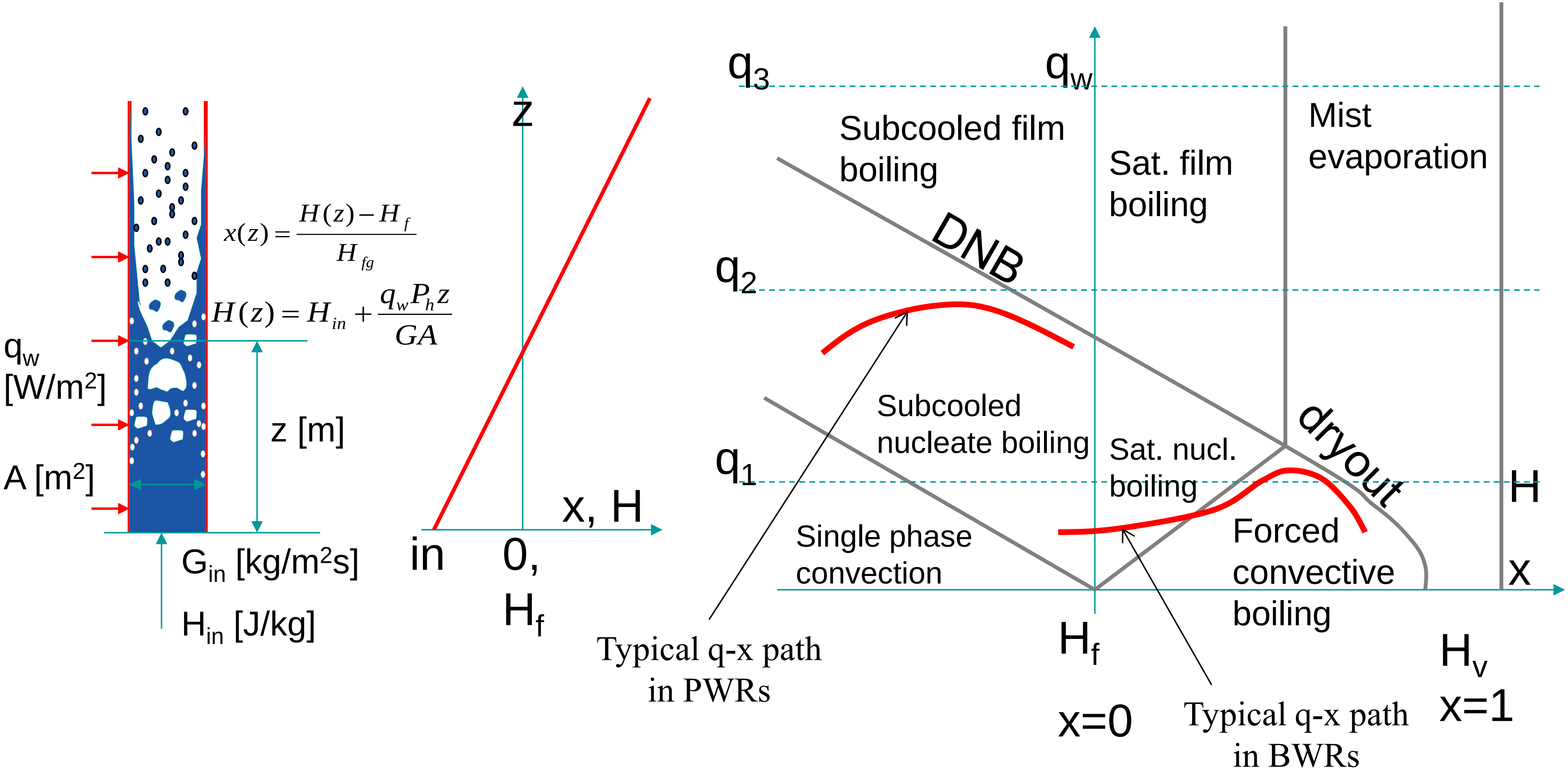

Experimentally observed DNB mechanisms

- Three major DNB mechanisms have been observed in experiments
  - Type 1: bubbly flow, where dry patches are created below single large bubbles
  - Type 2: DNB in bubbly microlayer under vapor clots
  - Type 3: DNB in liquid film under vapor slugs

Type 1 DNB – bubble grow

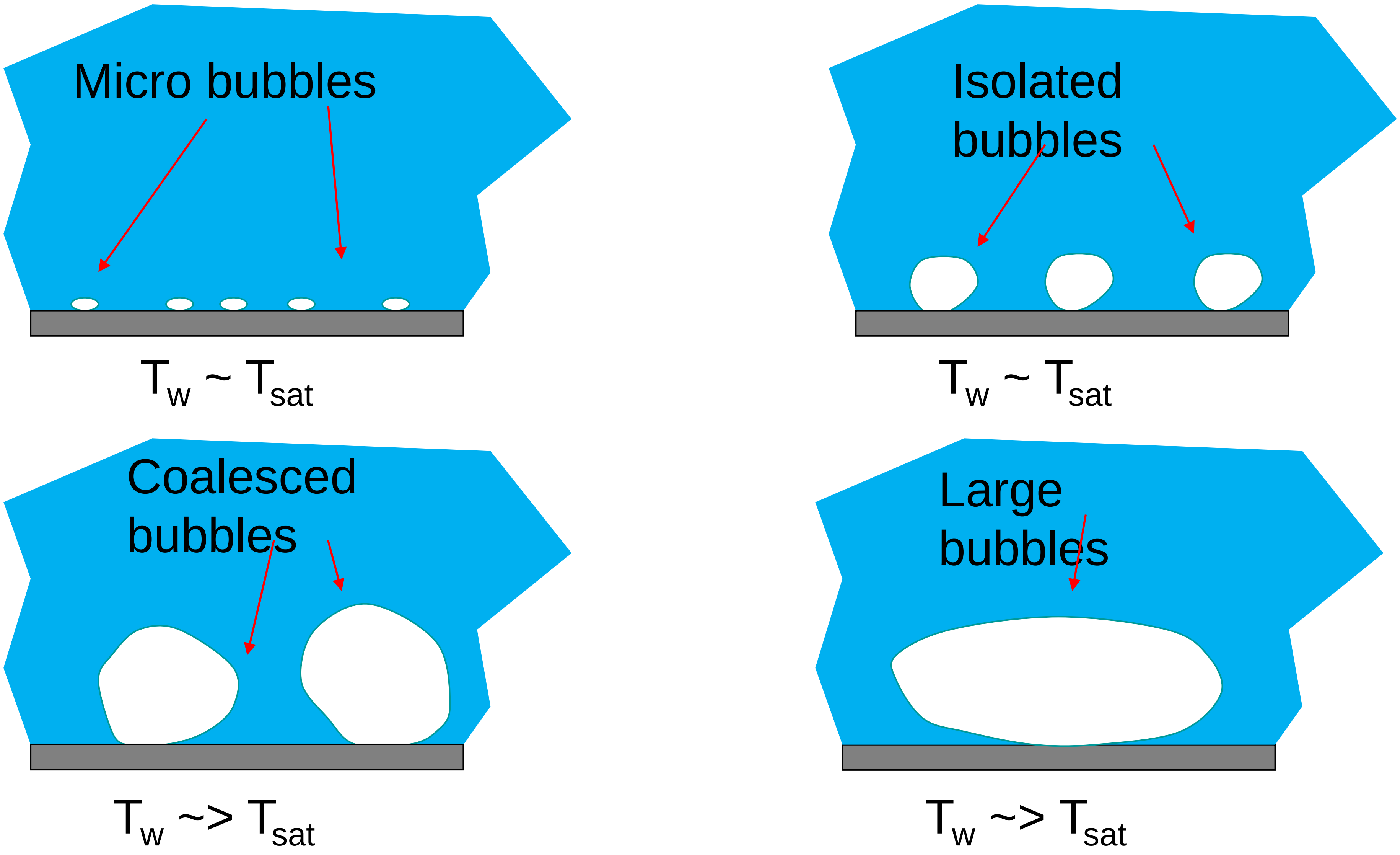

Type 1 DNB – towards crisis

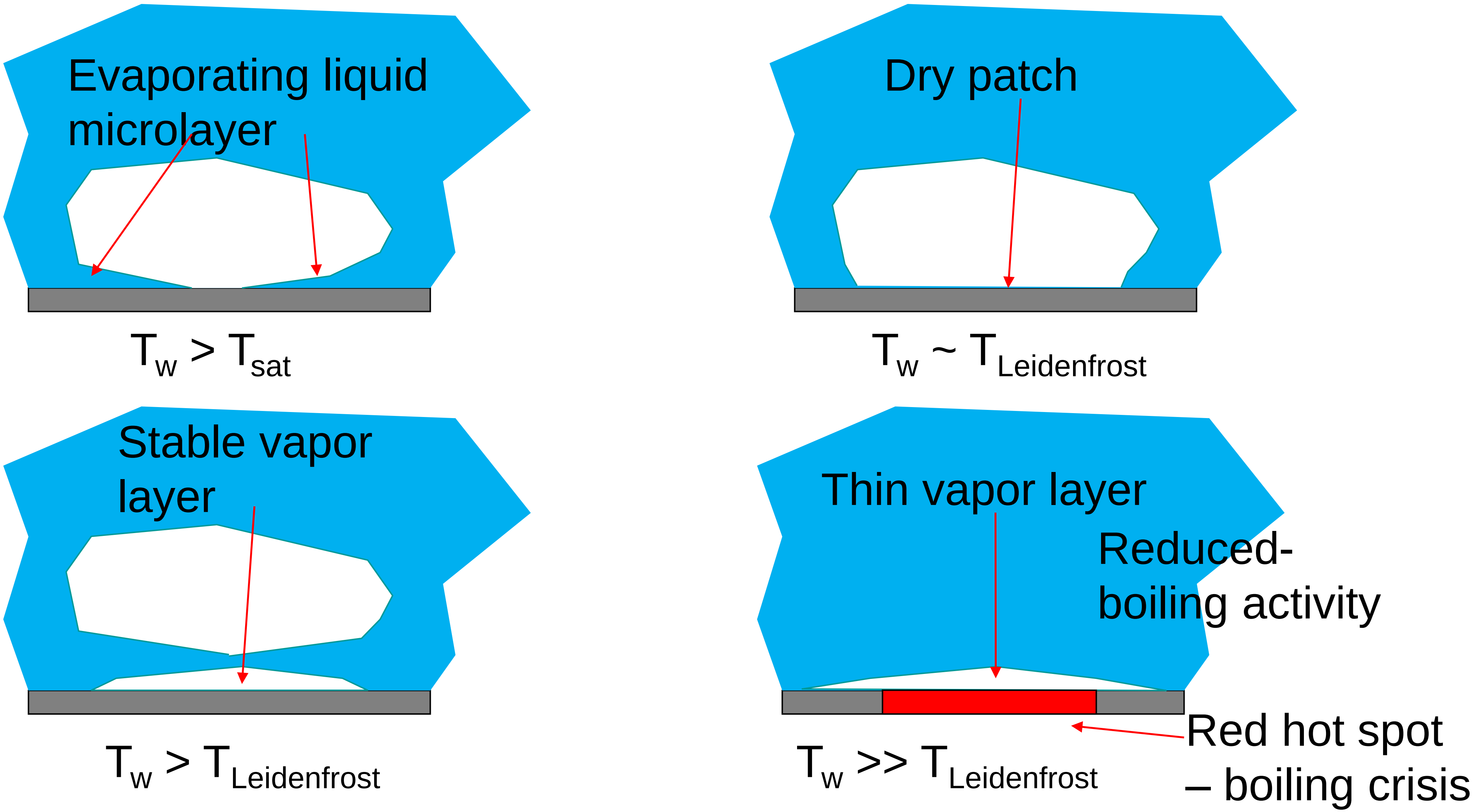

Type 1 DNB – visualization

CHF location

Melting-through heater

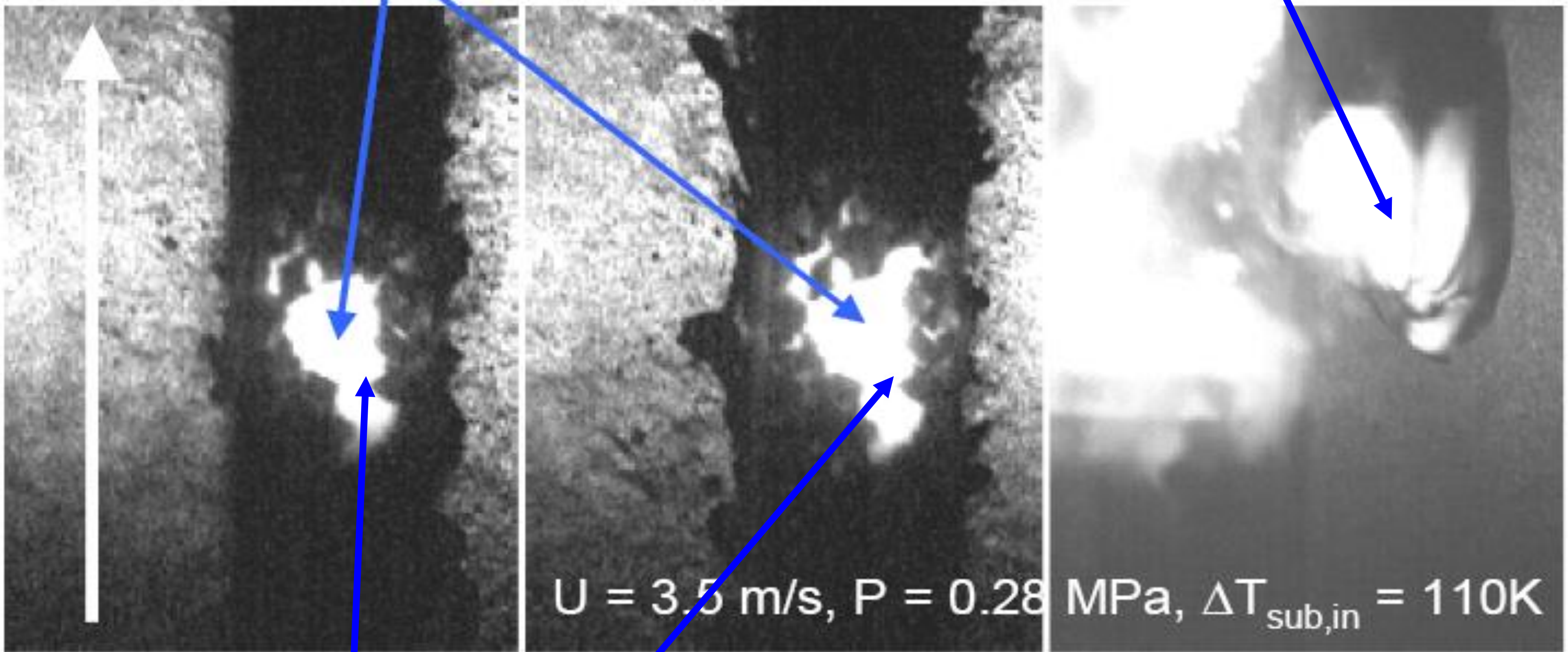

From Celata *et al.*, *Rev. Gén. Therm.* (1998)

Red and white metal

Type 2 DNB – bubble grow

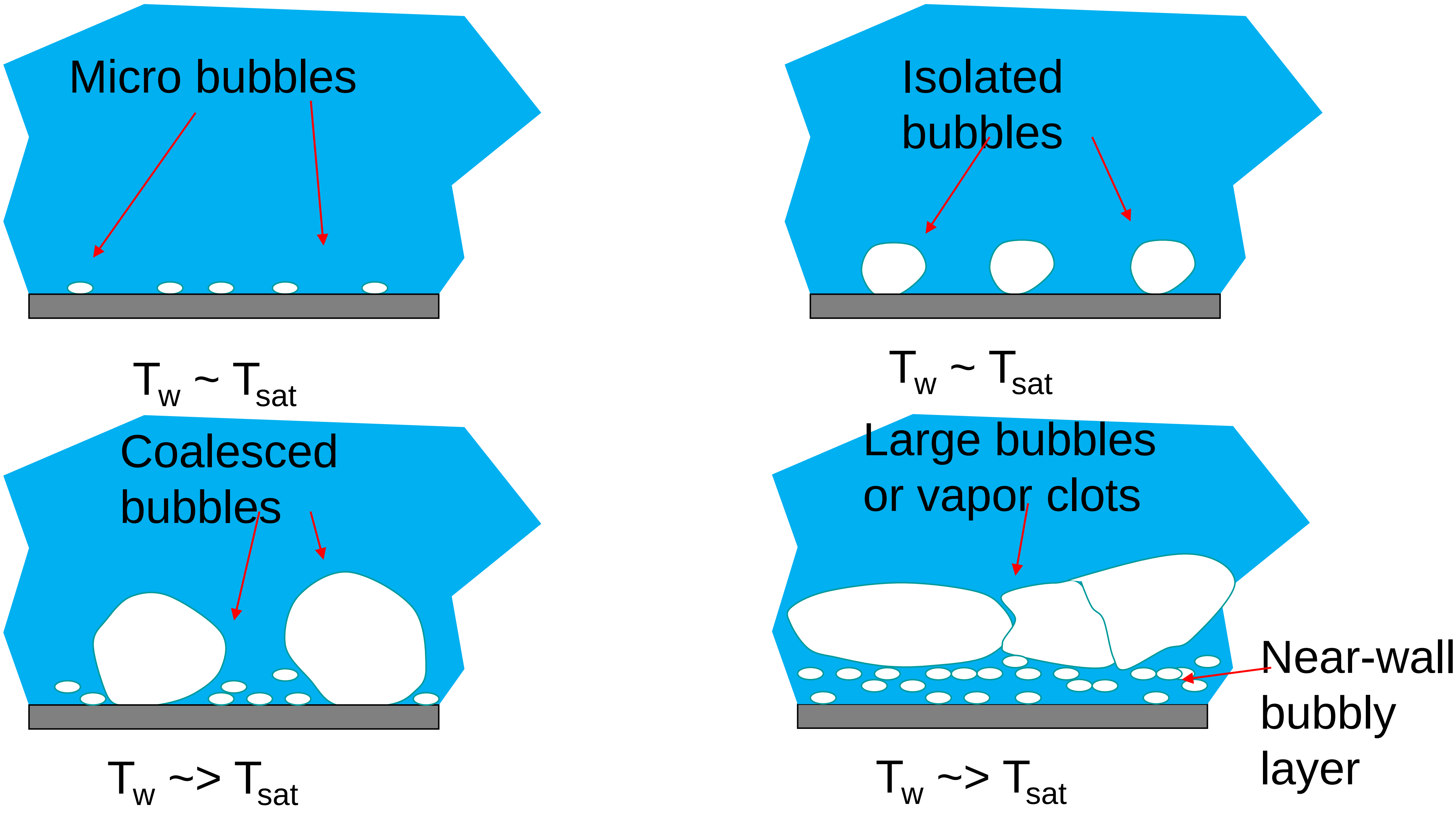

Type 2 DNB – evaporating bubbly layer

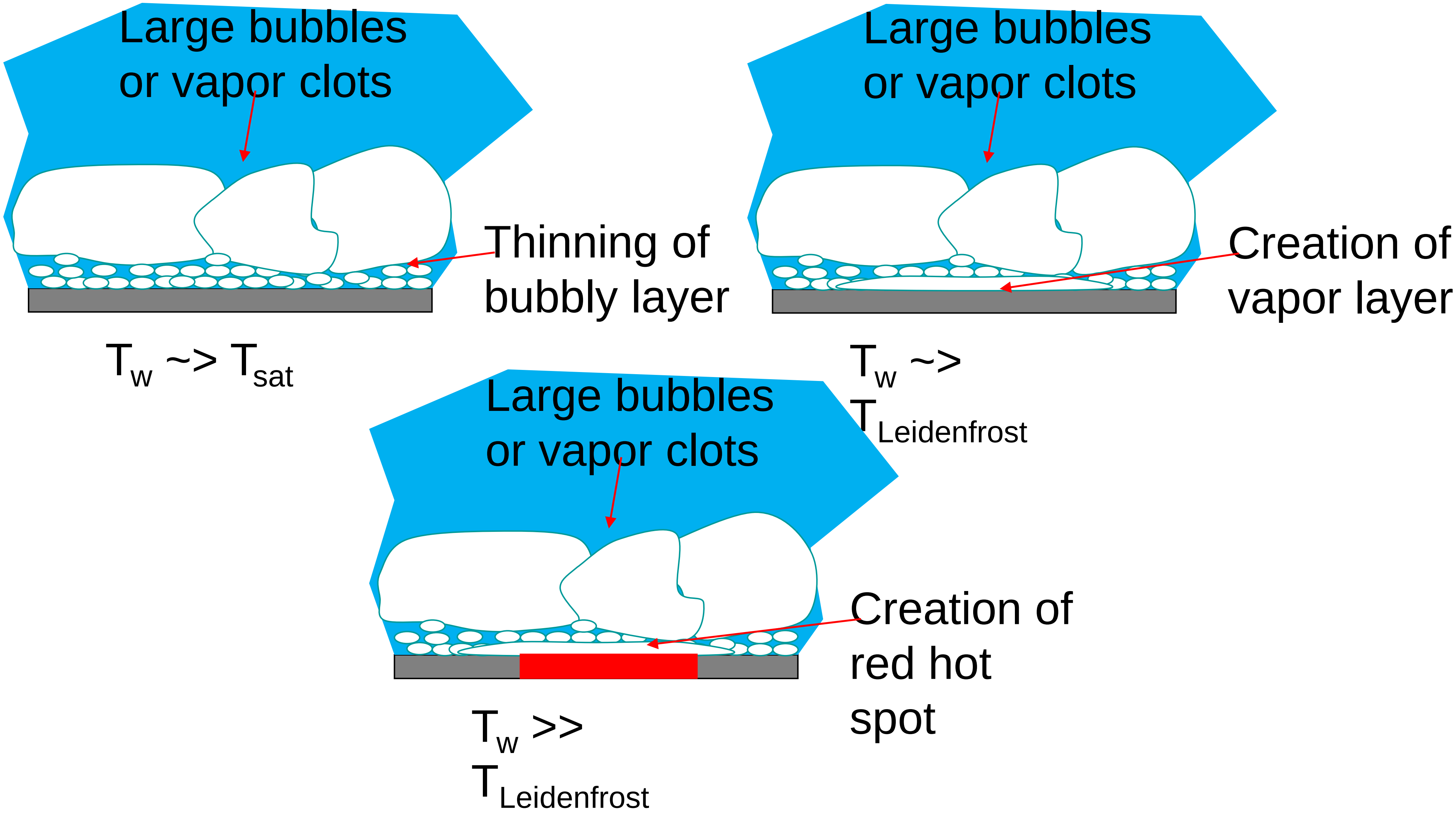

Type 2 DNB – visualization

From Bang *et al.*, *Int. J. Heat. Mass Transfer (2004)*

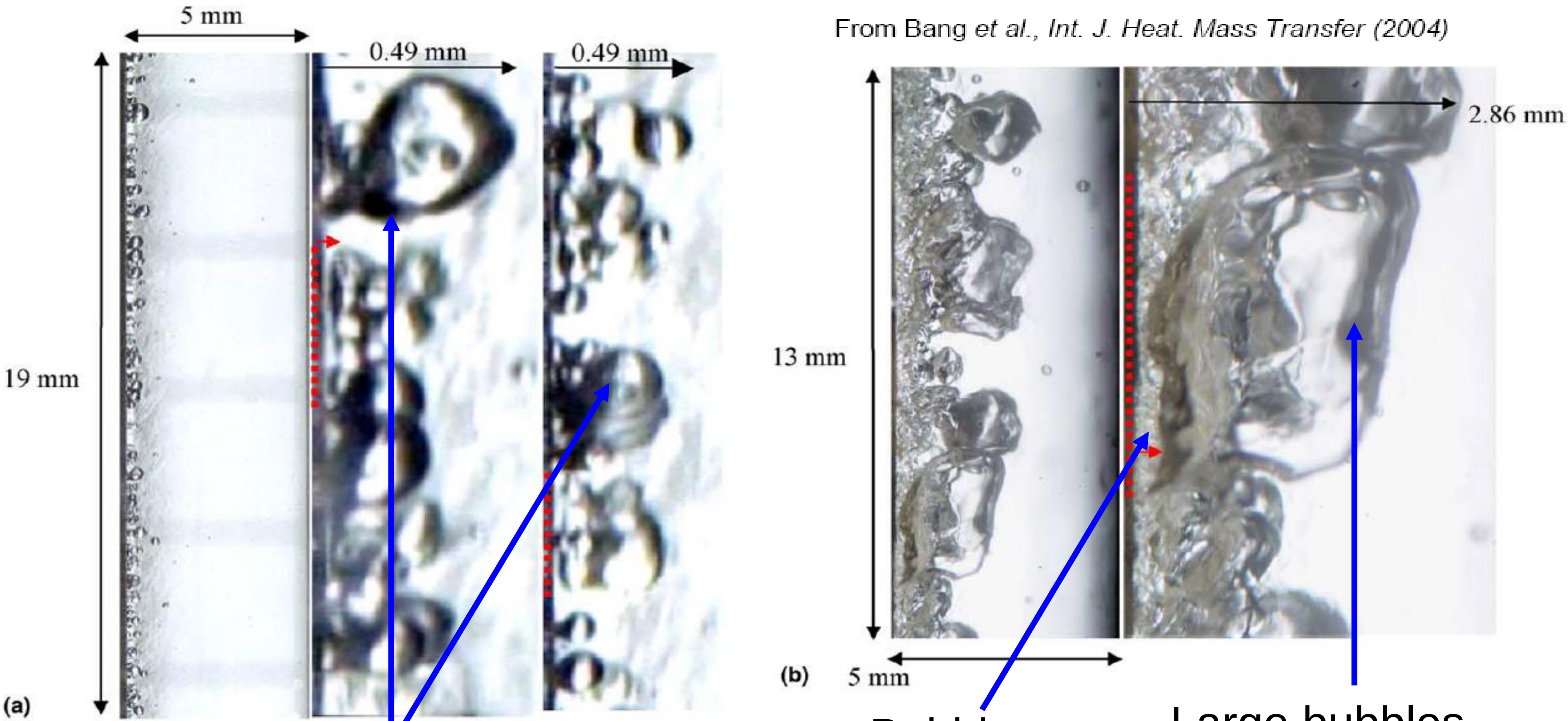

Small isolated bubbles

Bubbly microlayer

Large bubbles and vapor clots

Type 3 DNB – slug flow

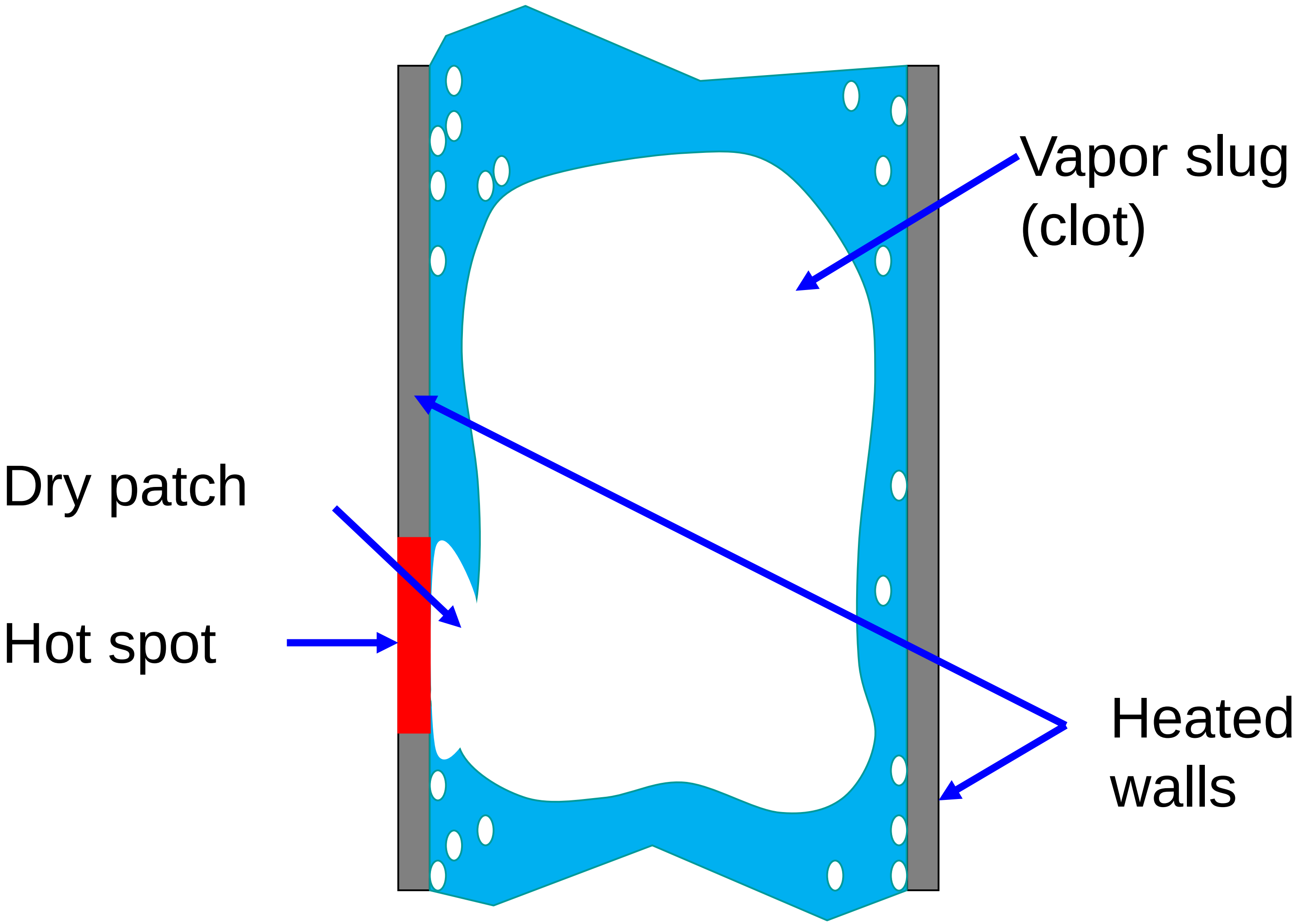

Type 3 DNB – visualization

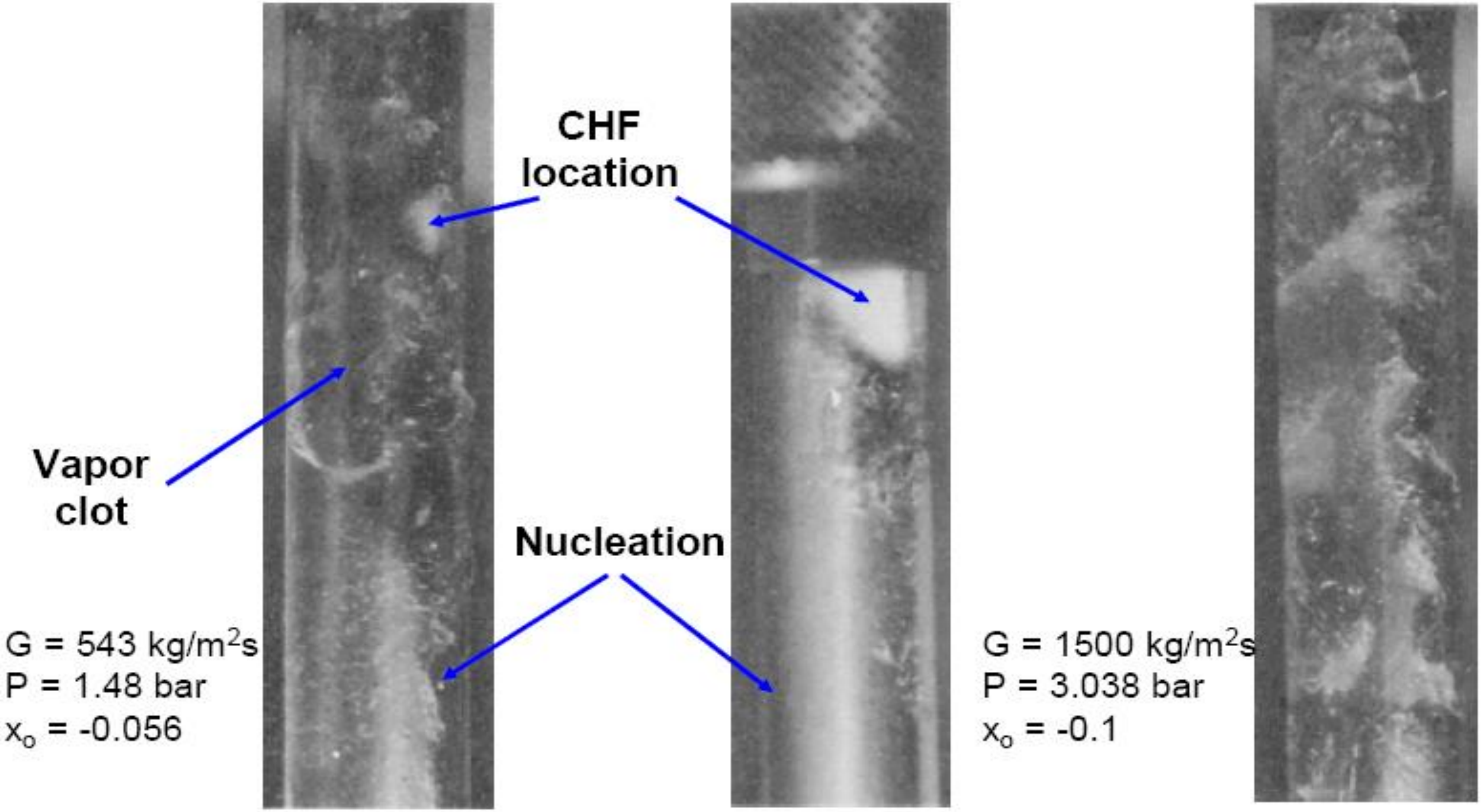

From Fiori and Bergles, *4th Int. Heat Transfer Conf. (1970)*

DNB We-x flow regime map

$$\mathrm{We} = \frac{G^2 D}{\rho_f \sigma}$$

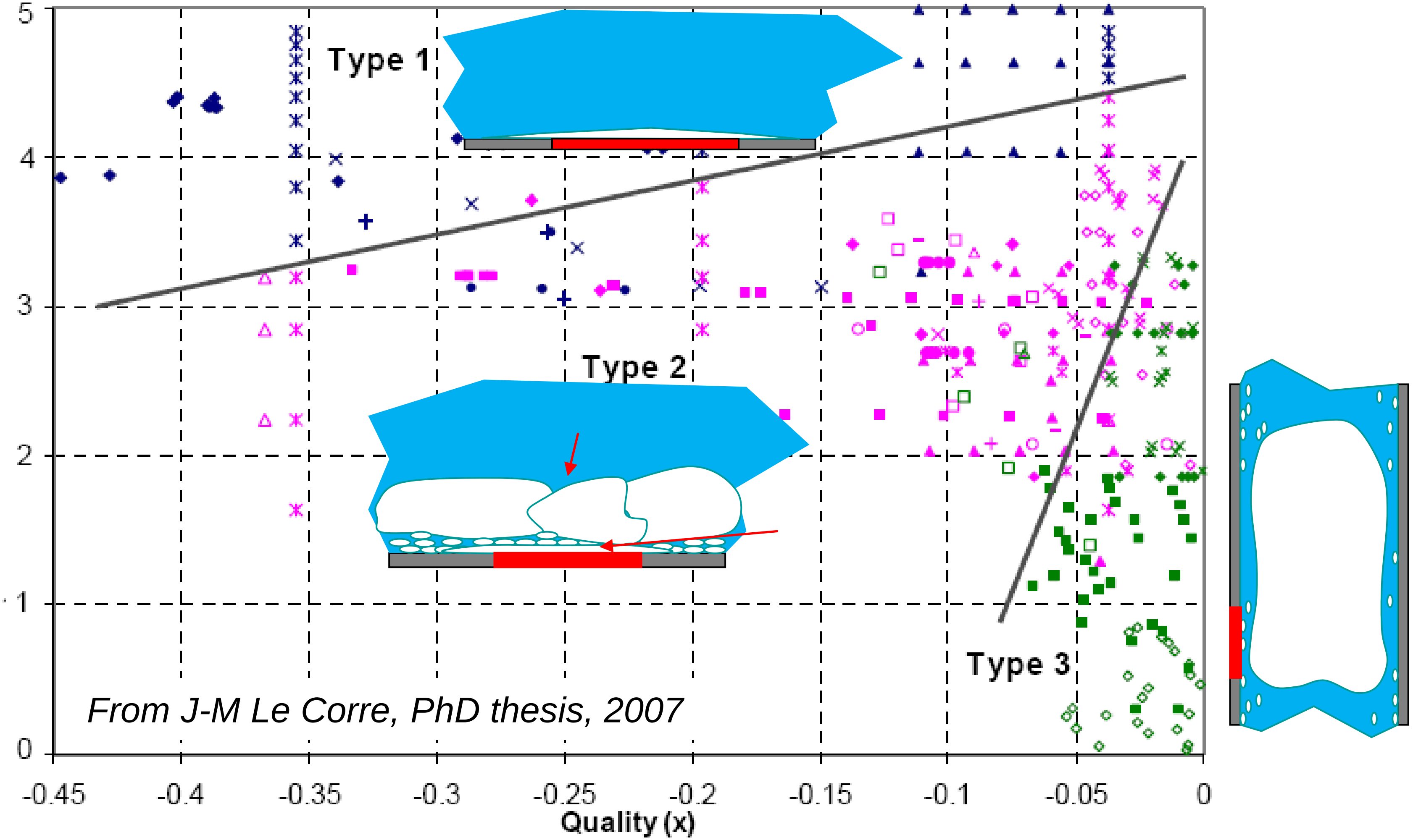

All three types of DNB can be represented on a Weber number – quality plane

Modelling DNB

- Major categories of DNB models
  - Bubbly layer models (e.g. “bubble crowding” model” by e.g. Weisman and Pei)
  - Liquid sublayer models (e.g. model by Lee and Mudawar)
  - Bubble-nucleation models (e.g. “dry spots formation model” by Ha and No, 2000, Bricard et al. and J-M Le Corre, 2007)

Bubble crowding model

- Bubbles are collecting close to the heated wall in a bubbly layer
- There is an interchange of mass end enthalpy between the bubble layer and the bulk flow
- DNB occurs when void fraction in the bubbly layer exceeds a critical value of 0.82
- At that point liquid is blocked and can not reach the wall

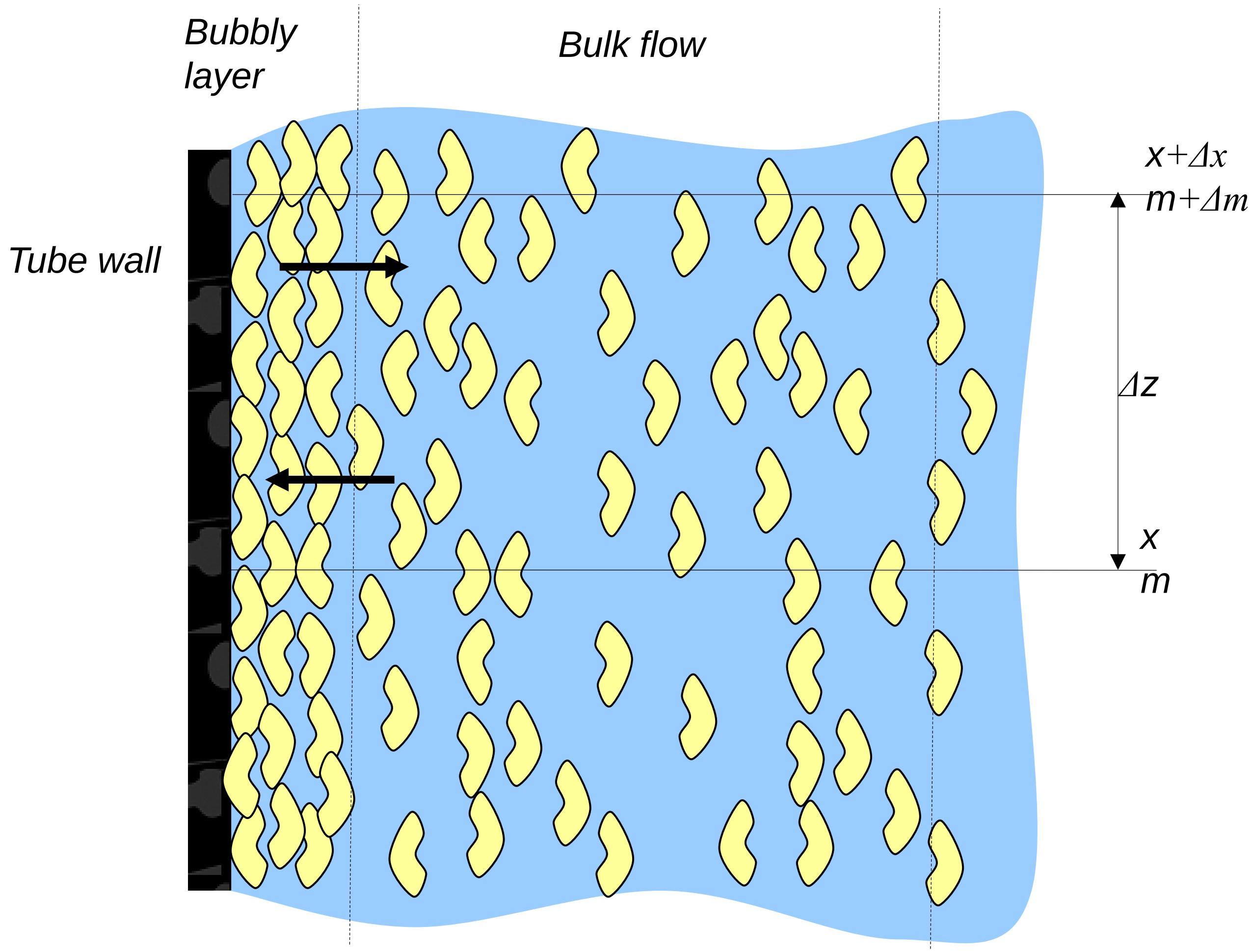

Liquid sublayer model

- Bubbles are collecting close to the heated wall
- Liquid film is created between the heated wall and the vapor blanket
- Vapor blanket becomes unstable due to Kelvin-Helmholtz instability
- Liquid film dries out and dry spots appear, leading to DNB

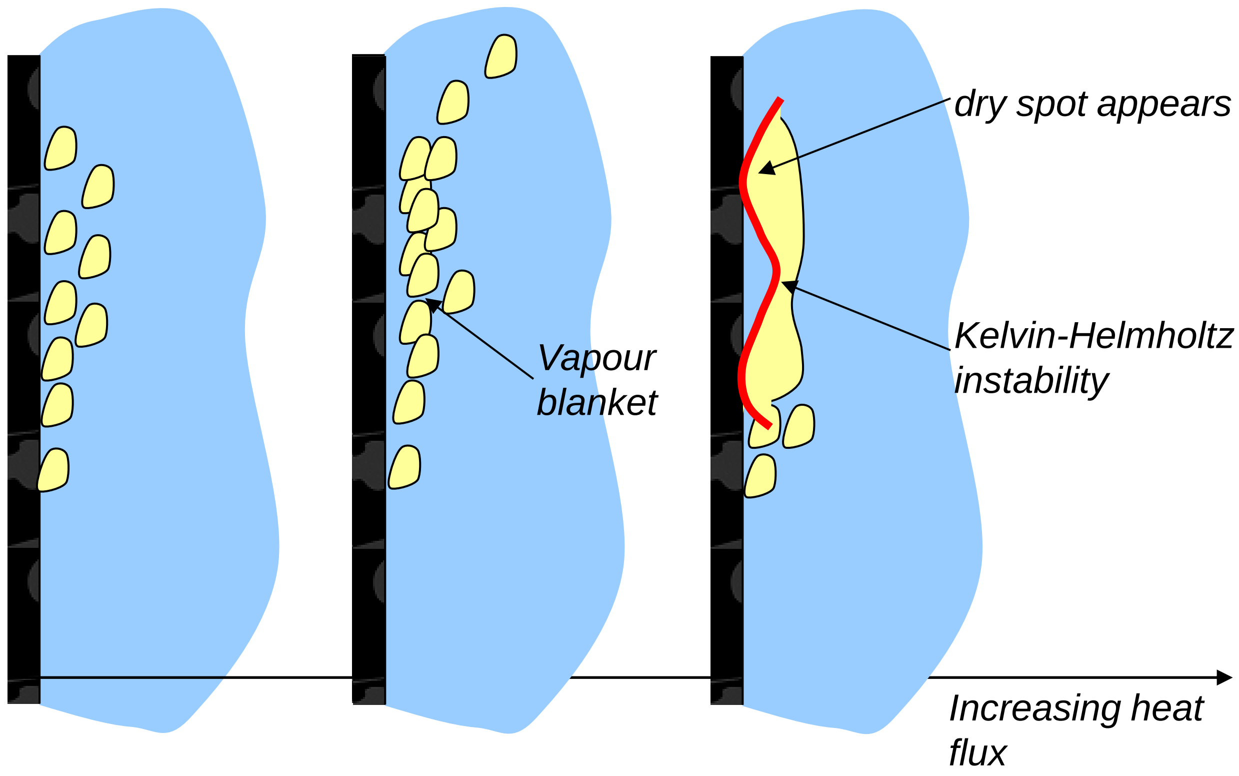

Bubble nucleation limit

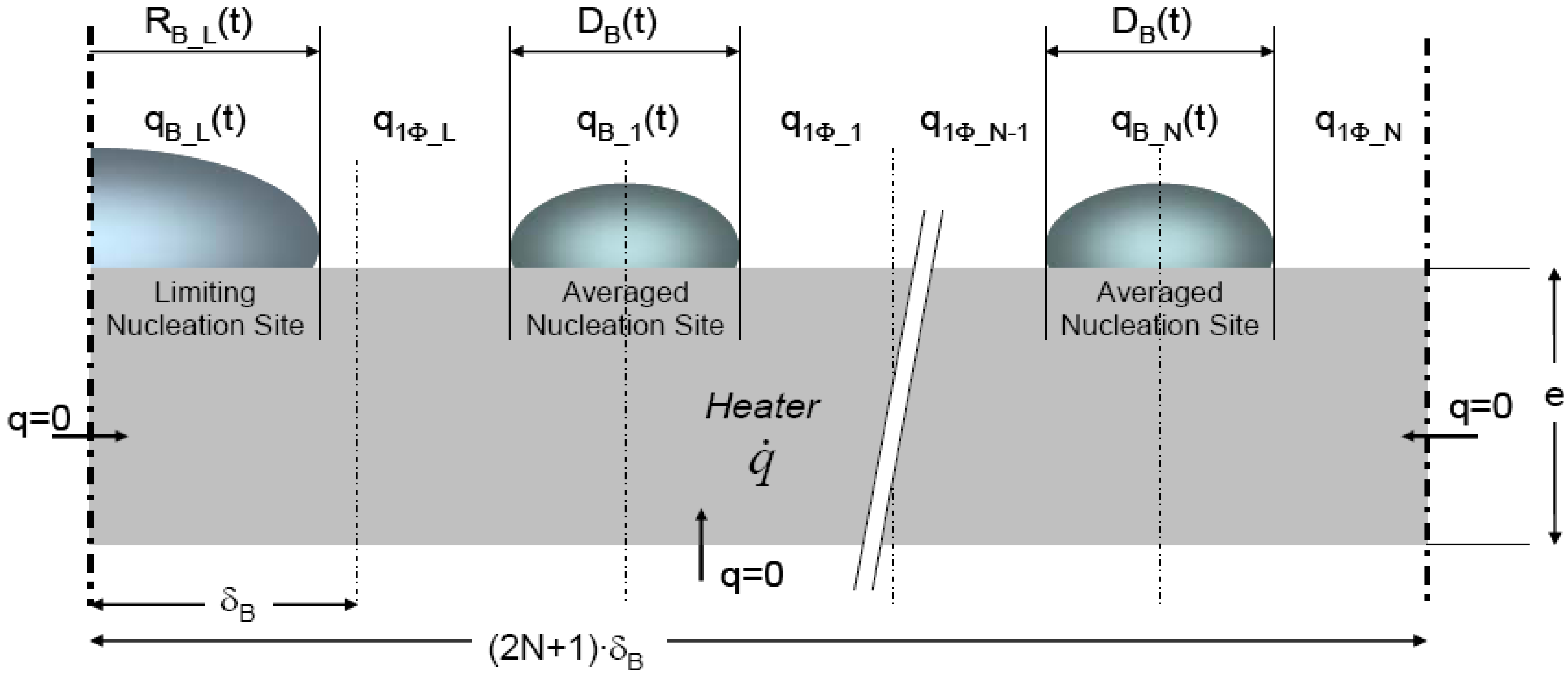

J-M Le Corre, 2007

Examples of CFD Models of DNB

- NEPTUNE_CFD approach (EDF, France)
  - two-fluid framework with drag, added mass, lift and turbulent dispersion forces
  - turbulent modelled with k-e and RSTM
  - bubble size distribution
  - wall function for boiling flow (Mamouni et al. 2009)
  - DNB criterion based on void fraction at the wall and the wall temperature
- PSI_BOIL approach (PSI, Switzerland)

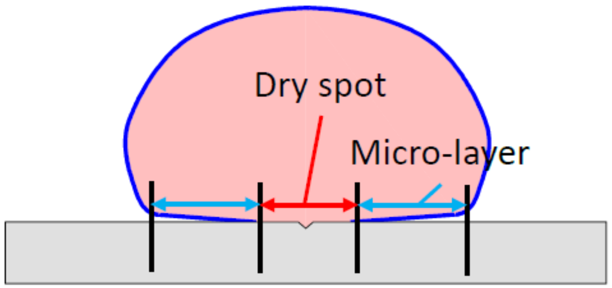

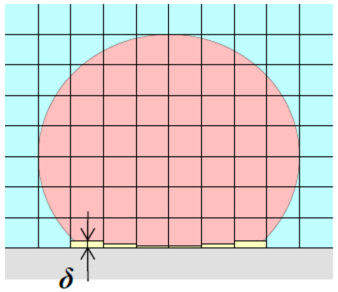

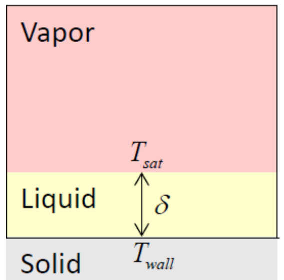

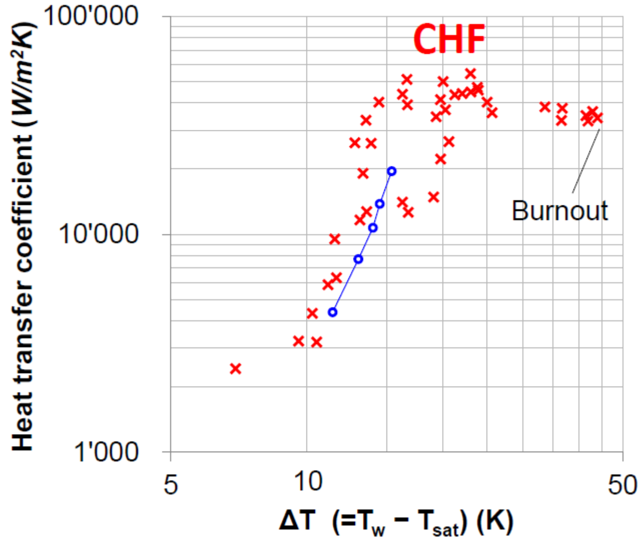

Sato and Niceno, JCP, 2015

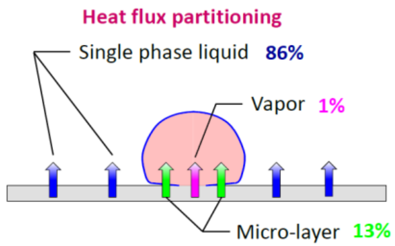

ROYAL INSTITUTE OF TECHNOLOGY

Experimental Investigation of Bubble Ebullition (Kromer, Anglart et al.,2016)

KTH

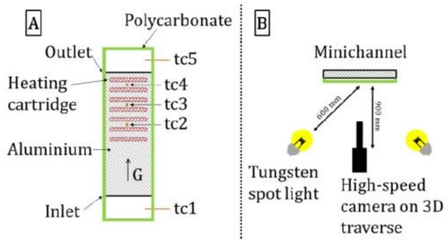

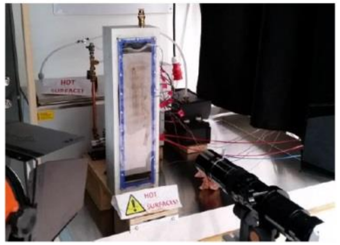

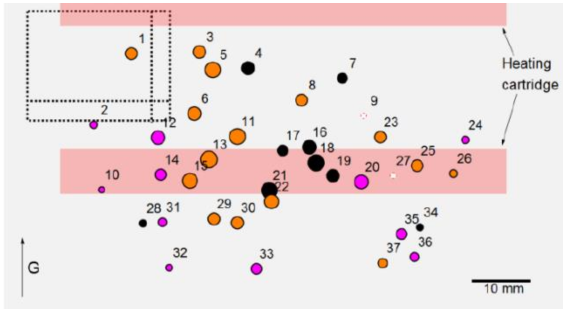

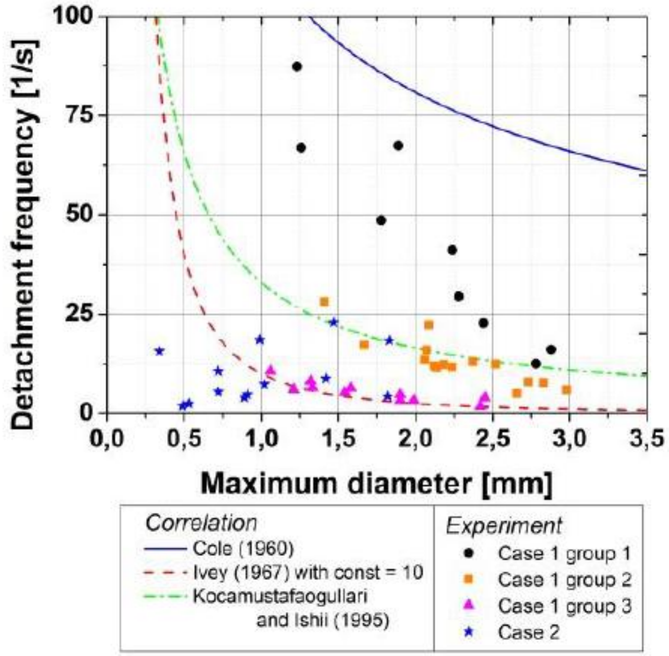

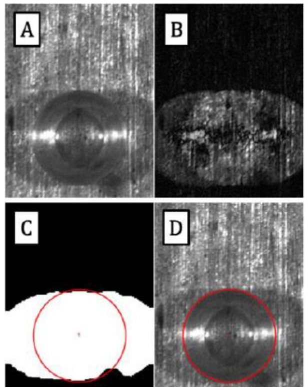

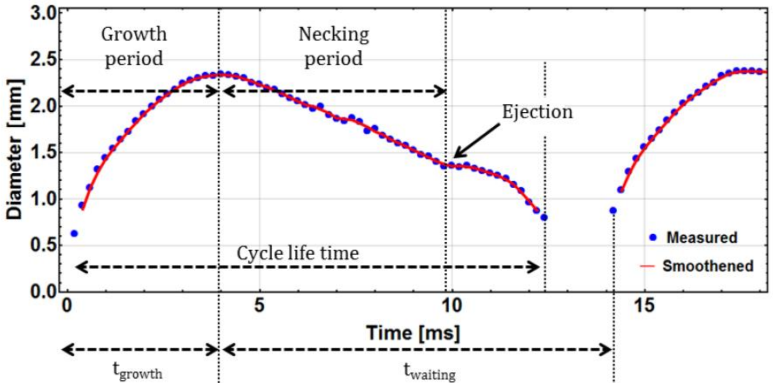

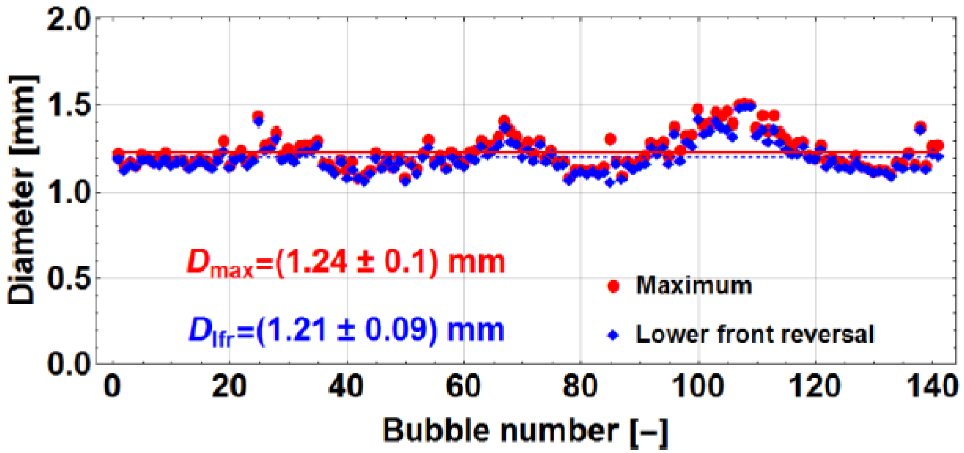

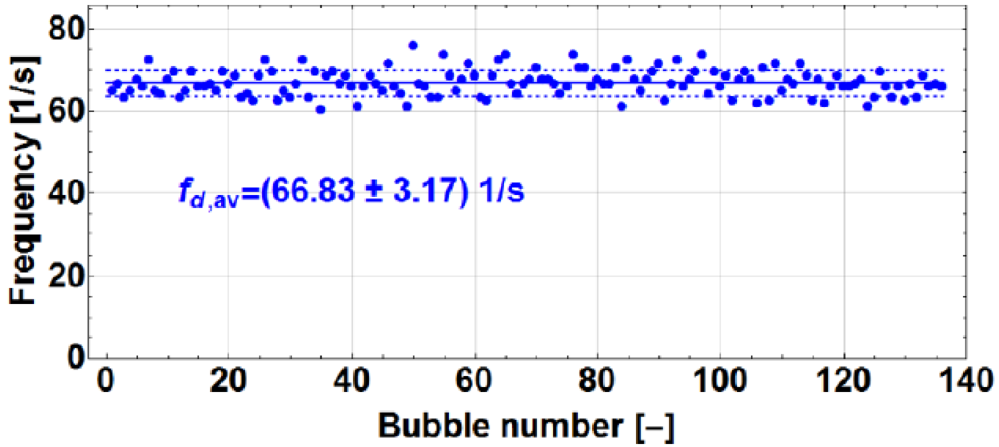

Main Open Questions in Modelling of Dryout

- Some of the closure laws are quite well developed and prove to give results that are in agreement with experiments; e.g. deposition rates and entrainment rates

- Other still require some fundamental development:

  - drop size in annular flow
  - the liquid film fraction at the onset of annular flow
  - the liquid film thickness at dryout

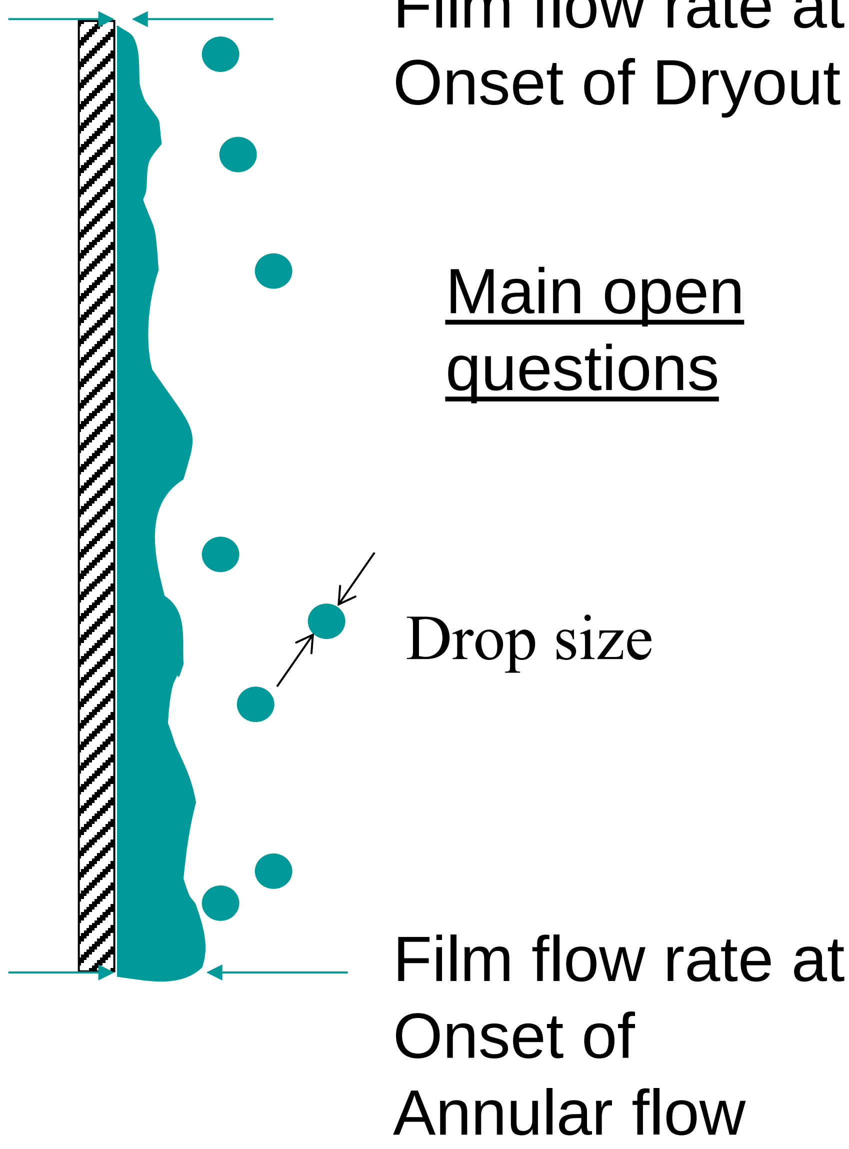

Recent Measurement of Droplet Size in Bundles

- New experimental data have been obtained recently
  - 3x3 BWR bundle
  - high speed camera recording
  - each pixel on image correspond to ~7μm
  - air - water
  - pressure: 117.1 – 146.5 kPa
  - temperature : 15 – 16 °C

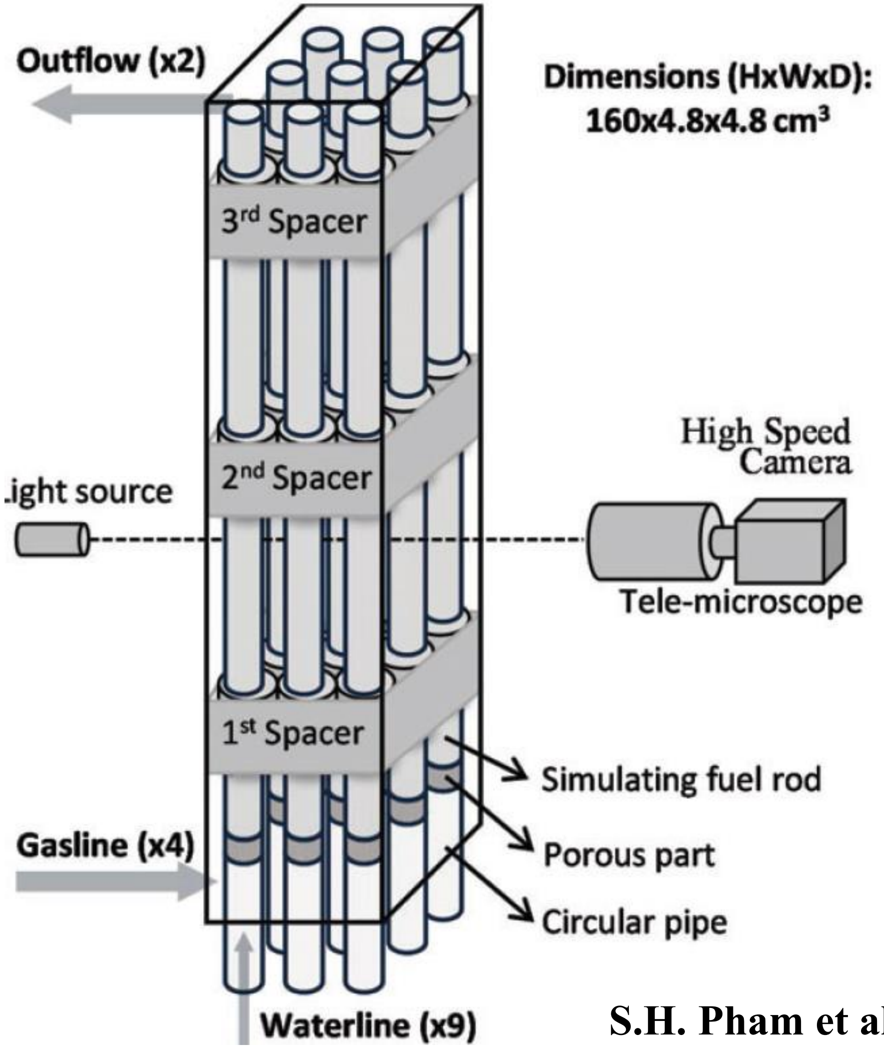

S.H. Pham et al., NURETH-16, 2015

Recent Measurement of Droplet Size in Bundles

- Figures show droplet size distributions 6 cm upstream of the spacer (lower figure) and 10 cm downstream of the spacer (upper figure)
- Note:
  - spacer introduces a huge number of small droplets
  - the peak size is at ~50 μm
  - a few large droplets (above 400 μm) appears downstream of the spacer (due to formation of thick ligaments on the top of the spacer)

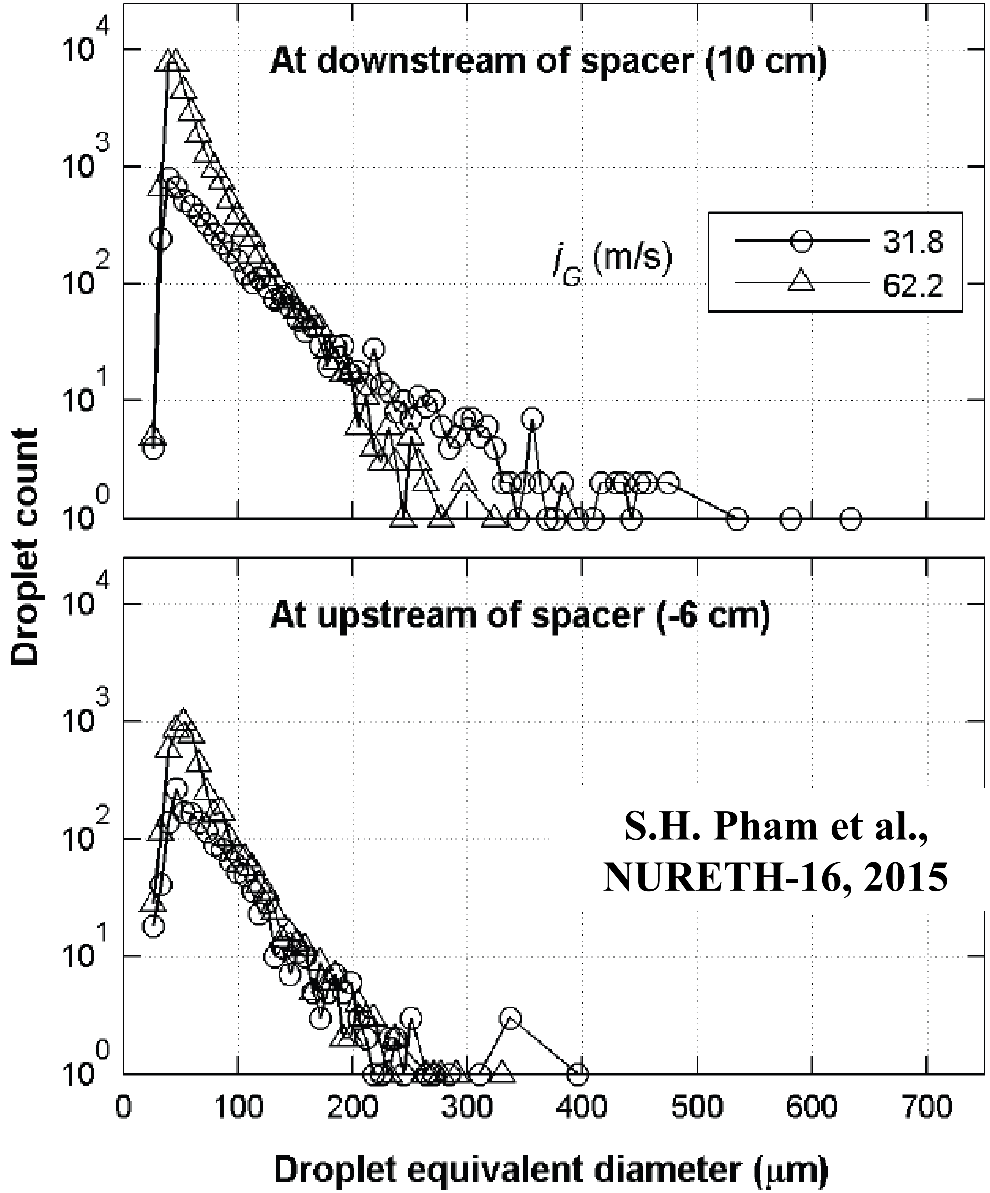

Measured Droplet Size Distributions at BWR Conditions

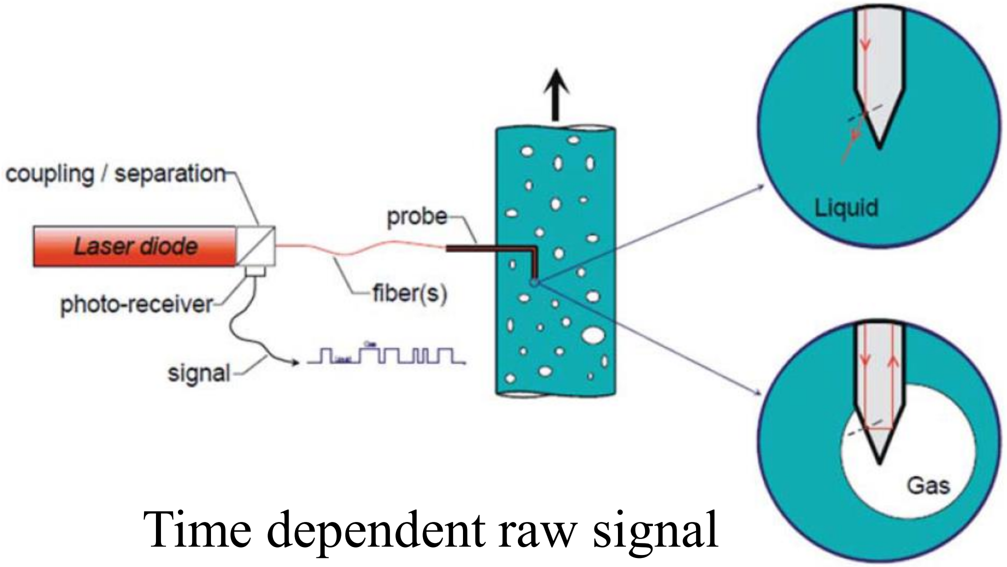

Time dependent raw signal

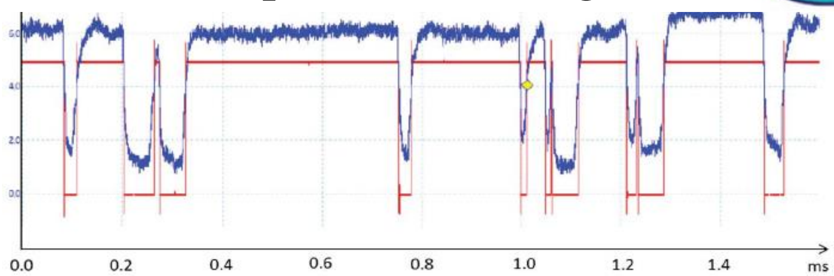

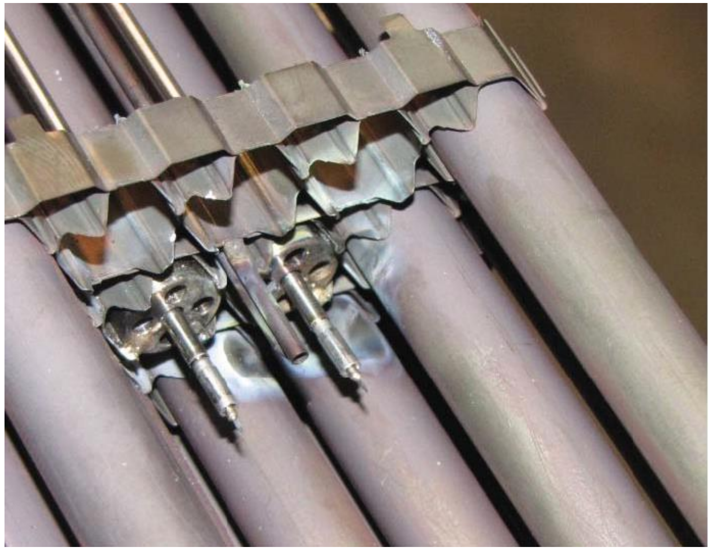

J.-M. Le Corre et al., NURETH-16, 2015

- Saphirre optical probe used in FRIGG for local void measurements
- Operation conditions: p = 7 MPa, T = 285 °C

Measured Droplet Size Distributions at BWR Conditions

- Measured drop size characteristics [mm]:
  - minimum 0.2
  - arithm. mean: 0.3
  - Sauter mean: 0.7
  - de Brouckere mean 1.2
  - maximum: 5.3
- Void fraction in the core: 0.9 – 0.99
- Flow velocity up to 35 m/s

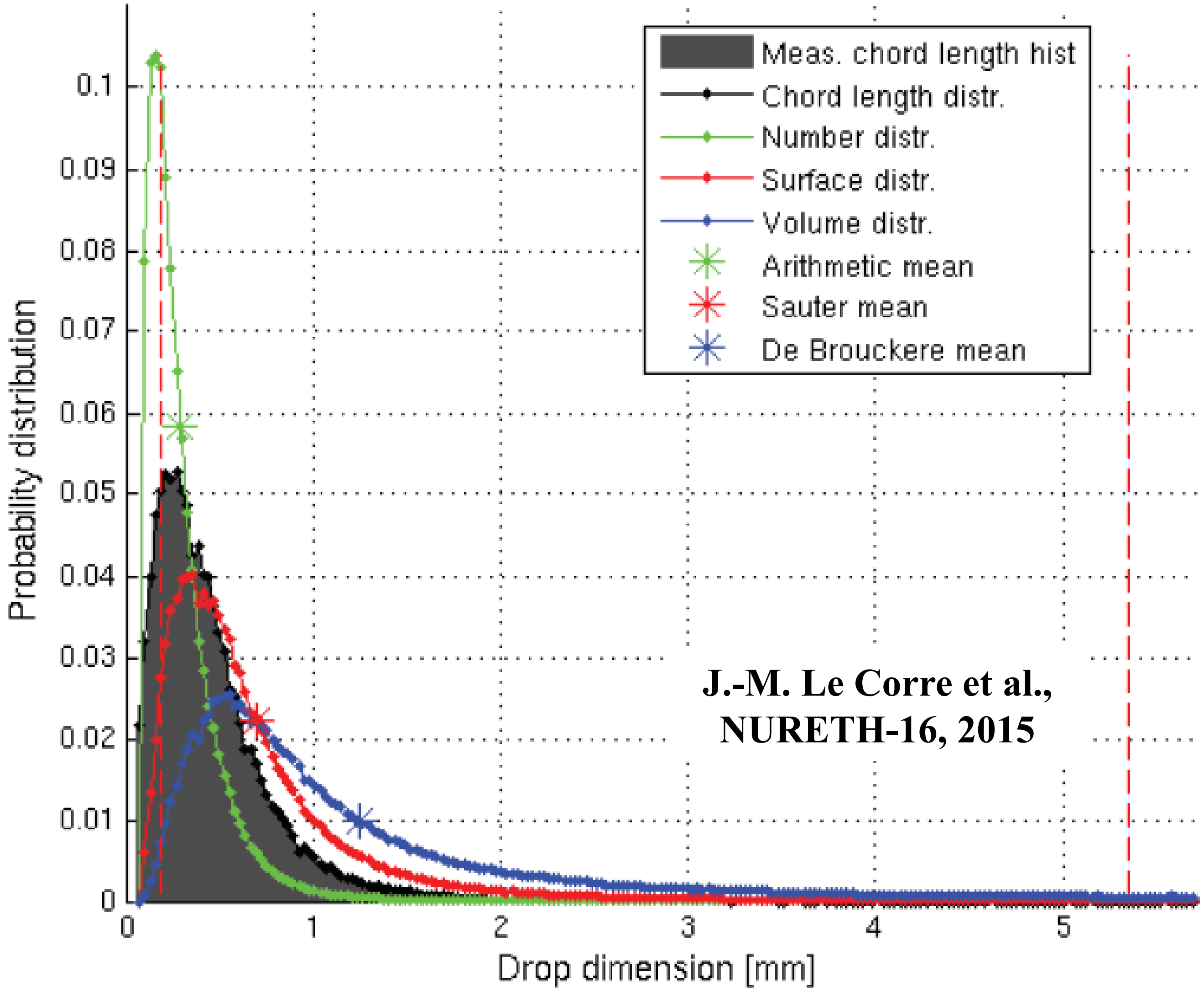

Turbulent Flow in Nuclear Fuel Assemblies with Spacer Grids

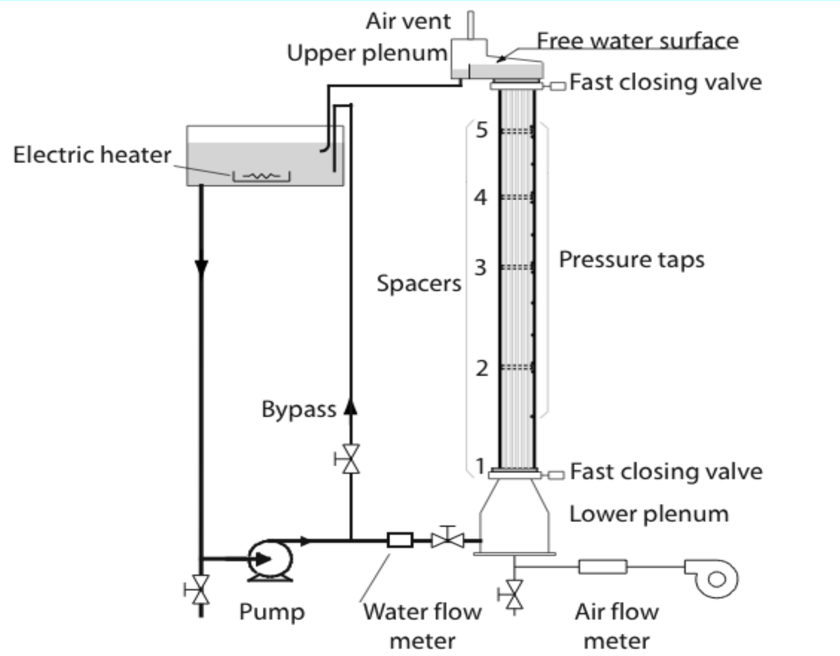

Water-air loop for thermal-hydraulic investigations in fuel assemblies

DETAILED LDV MEASUREMENTS

Turbulence intensity downstream of a spacer grid (*Caraghiaur, Anglart, Frid, NED,* 2009)

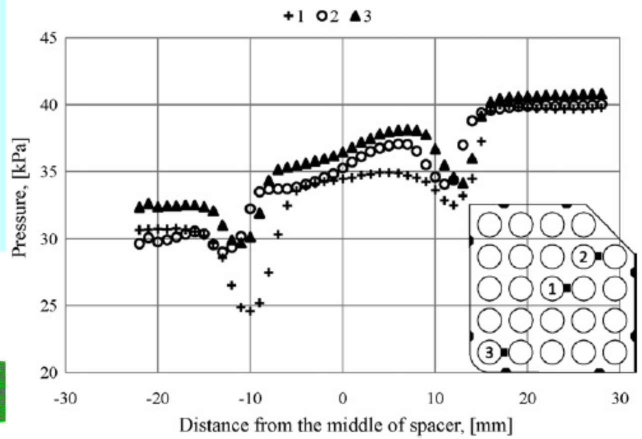

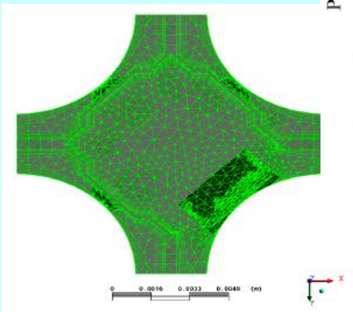

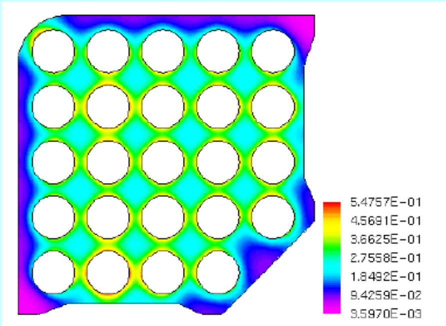

New multi-phase CFD models for nuclear applications developed

Lateral Distribution of Spacer Effect on Turbulence in a Rod Bundle

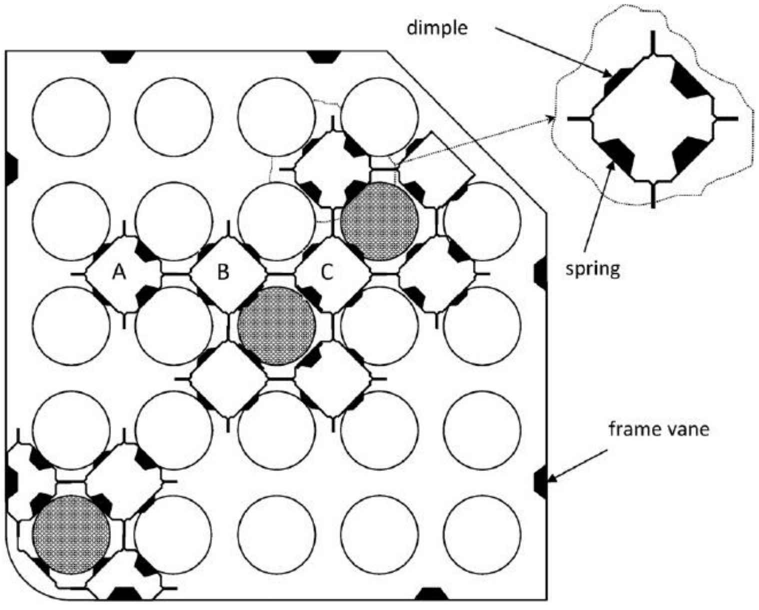

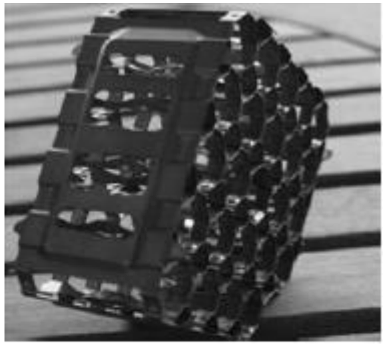

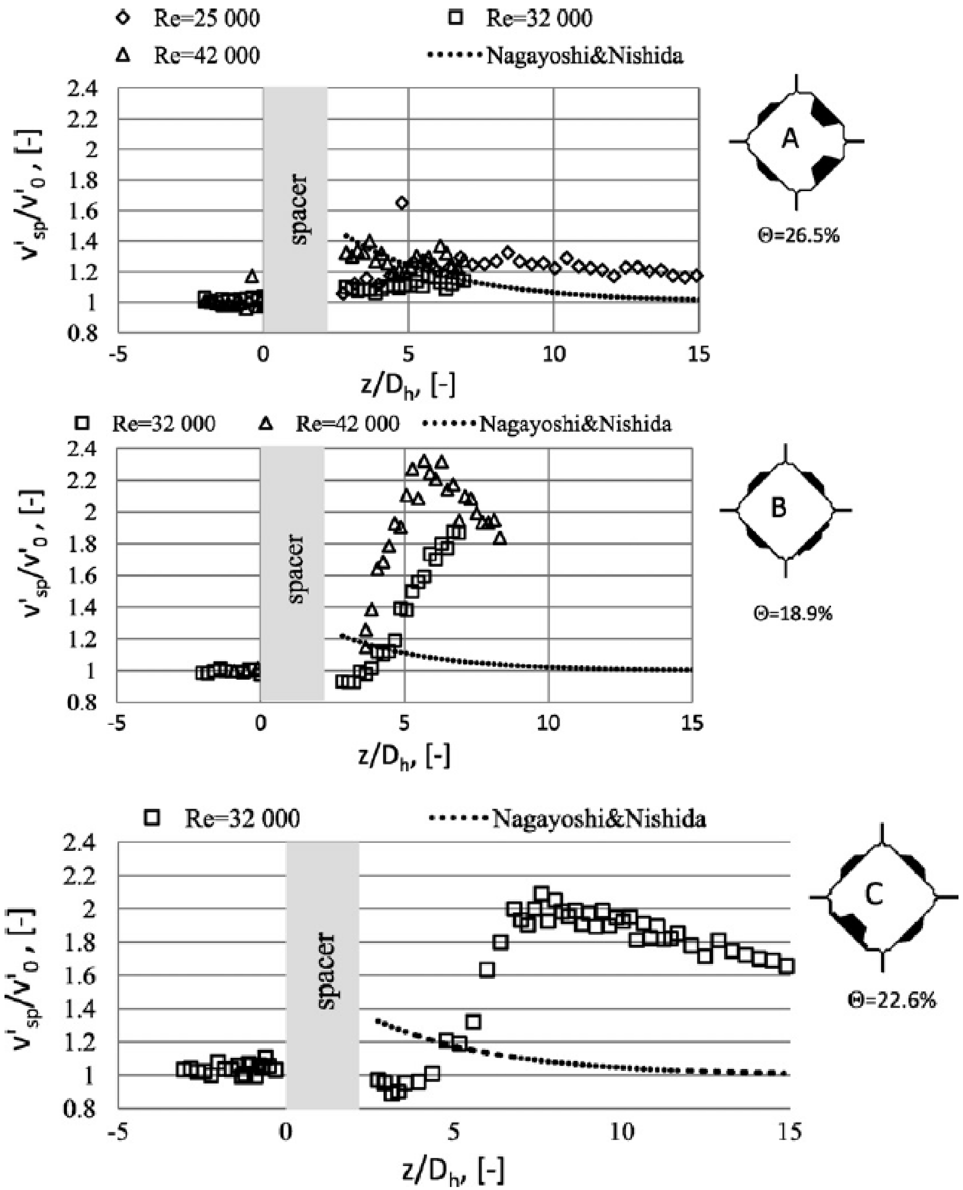

Caraghiaur et al. *NED*, 2010

Approach to Dryout using CFD

- Mechanistic approach to model dryout should relay on the basic conservation laws for mass, momentum and energy

- This approach has an advantage of most general applicability and high accuracy

- Deposition rates are obtained from detailed particle-tracking analyses using CFD

- Entrainment rates are obtained from models based on liquid film instability

- This approach requires adequate closure laws and sub-grid models which are not available yet

Early CFD Models

- The basic idea in this model was to predict the liquid film thickness on heated rods

- Eulerian-Eulerian approach to gas core + 1D liquid film model

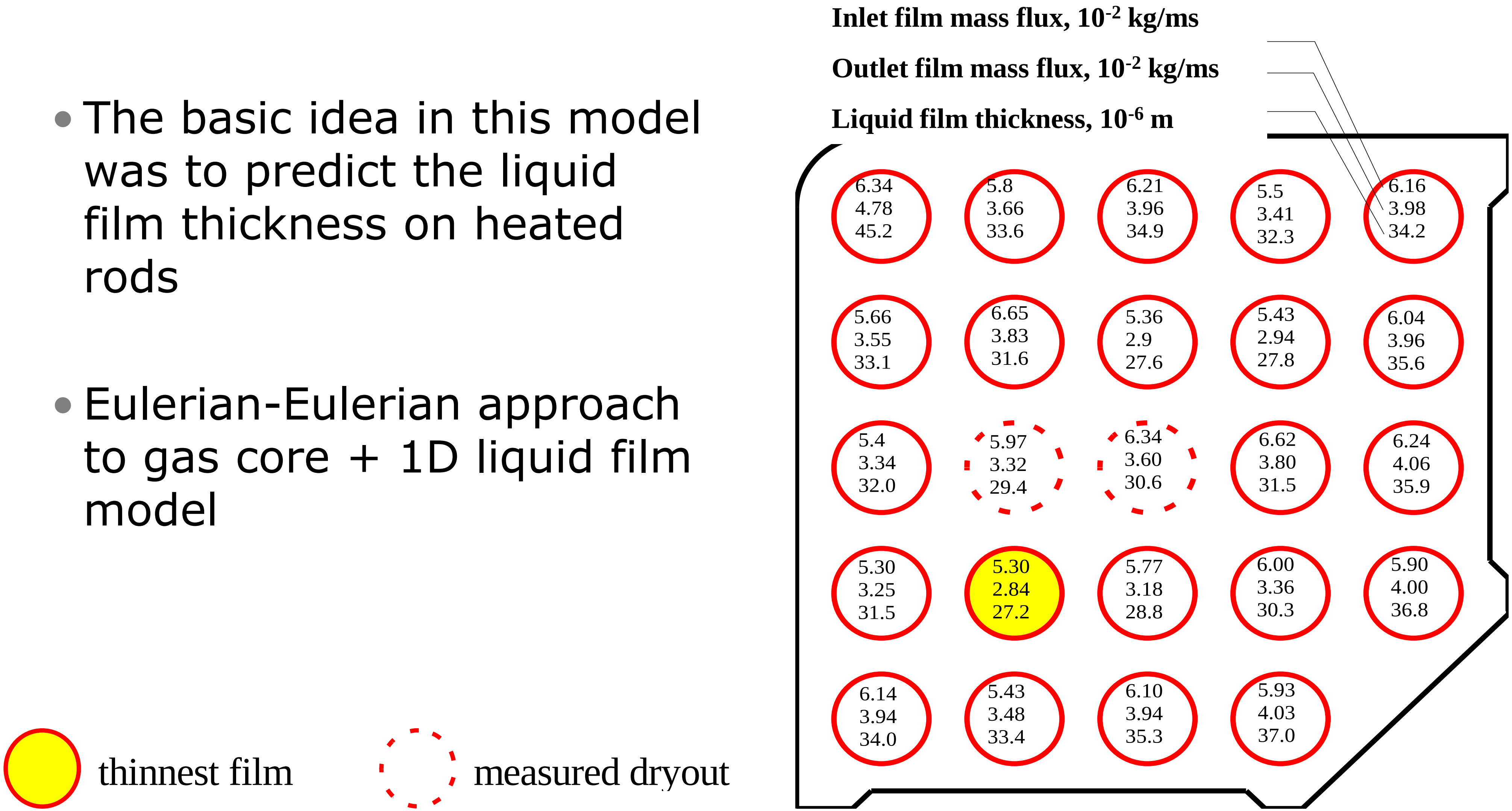

Anglart et al. (1998)

Current CFD Modelling of Annular Mist Flow - Liquid Film Model

- Eulerian-Lagrangian approach with liquid film capability (Li and Anglart, ANE, 2015)
- Basic assumptions for thin liquid film model:
  - flow in normal direction to wall is neglected
  - advection is treated in wall tangential direction only
  - difussion is treated in wall normal direction

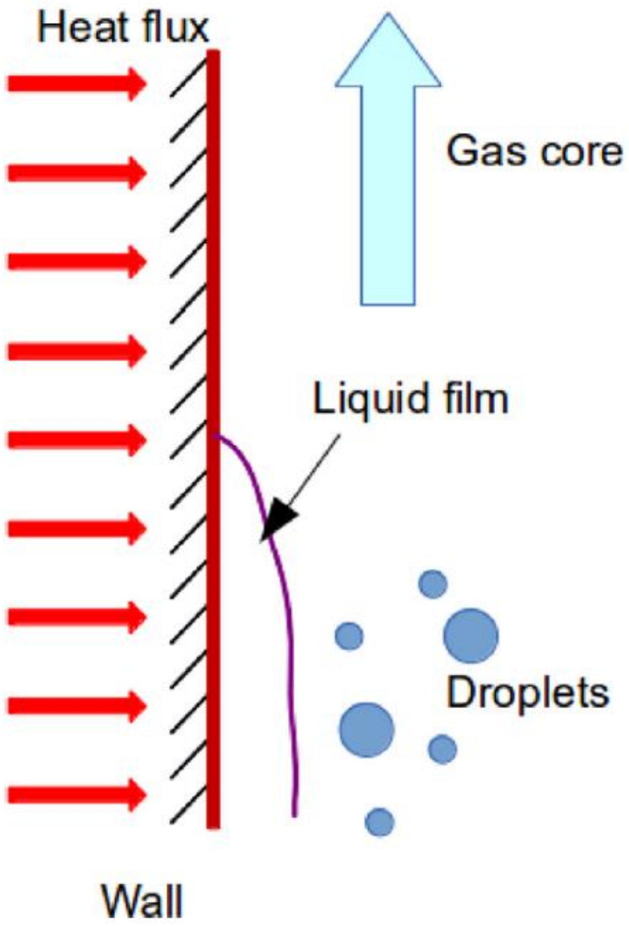

CFD Modelling of Annular Mist Flow Liquid Film Model

- The transport equation for the liquid fil can be integrated in the wall normal direction to give 2D equations
- All film properties are depth-averaged as follows

$$\bar{\phi} = \frac{1}{\delta}\int_0^\delta \phi dz$$

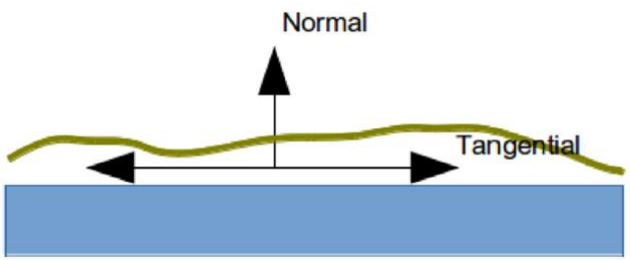

- The film conservation equations become

$$\frac{\partial(\rho\delta)}{\partial t} + \nabla_s \cdot (\rho\delta\mathbf{U}) = S_\delta$$

$$\frac{\partial(\rho\delta\mathbf{U})}{\partial t} + \nabla_s \cdot (\rho\delta\mathbf{U}\mathbf{U}) = -\delta\nabla_s p + S_\mathbf{U}$$

$$\frac{\partial(\rho\delta h)}{\partial t} + \nabla_s \cdot (\rho\delta h\mathbf{U}) = S_h$$

U - mean film vel. vect.,

h – mean film enthalpy,

δ – mean film thickness

Liquid Film Model
Mass Conservation

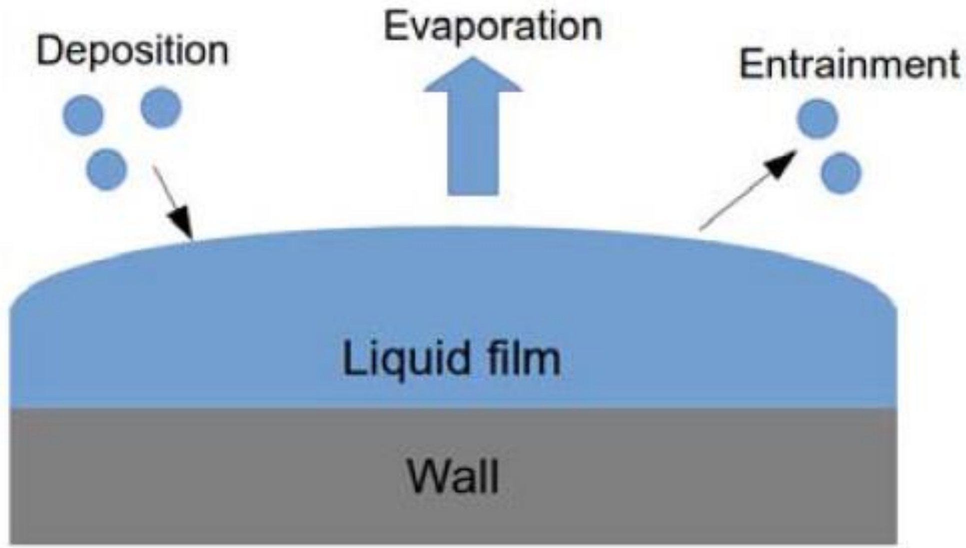

- Mass exchange between liquid film and gas core

- The evaporation rate is calculated from the mass/energy conservation at the interface

$$S_{\delta,evap} = -\frac{q''_w}{h_{fg}}$$

- The deposition rate is found from particle tracking (Euleriand-Lagrangian approach) or from correlations (Eulerian-Eulerian approach)
- The entrainment rate is found from correlations

Liquid Film Model
Momentum Conservation

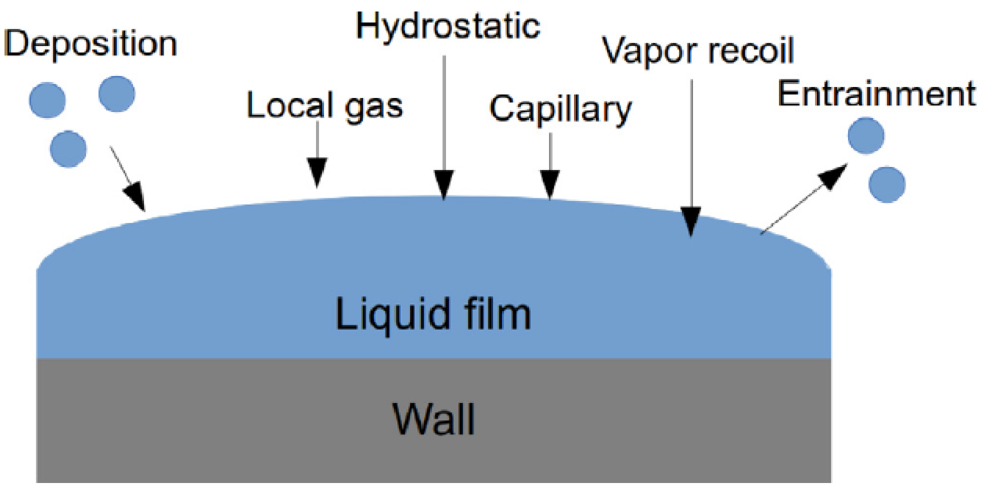

- Hydrostatic $p_\delta = -\rho\delta \mathbf{n} \cdot \mathbf{g}$
- Deposition $p_{dep} = \dot{m}_{dep}(\mathbf{v}_d \cdot \mathbf{n})$
- capilary $p_\sigma = -\sigma\nabla_s^2\delta$
- vapor recoil $p_{vap} = \dfrac{\rho_v |\mathbf{v}_v \cdot \mathbf{n}|^2}{2}$

- Momentum source terms for the liquid film in the film normal direction

Liquid Film Model
Momentum Conservation

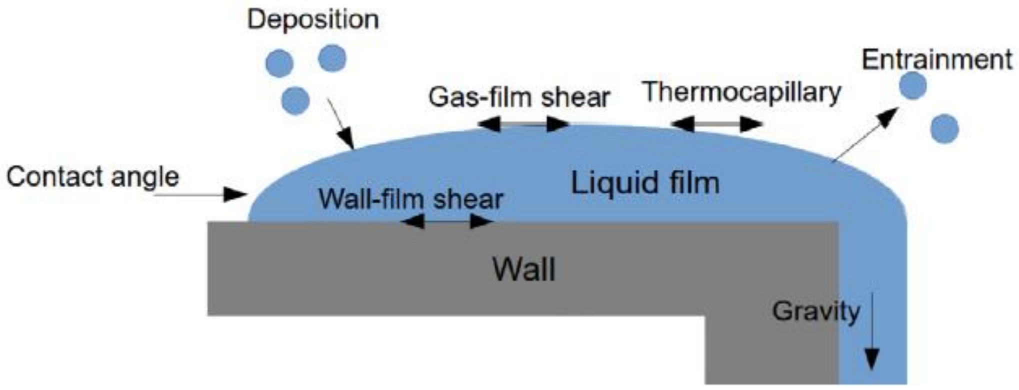

- Momentum source terms for the liquid film in the film tangential direction
- Thermocapillary $S_{\mathbf{U},mag} = -\nabla_s \sigma$
- Contact angle $F_c = \sigma(1 - \cos\theta)$
- Deposition $F_{\mathbf{U},dep} = \dot{m}_{dep} v_{dt}$
- Hydrostatic $S_{\mathbf{U},\delta} = \rho \delta g_t$
- Wall shear $S_{\mathbf{U},\tau_w} = -\mu_l \left(\frac{\partial \mathbf{u}}{\partial z} \right)_{z=0}$
- Interface shear

$$S_{\mathbf{U},\tau_g} = \frac{1}{2} C_{f,i} \rho_g \left| \mathbf{u}_g - \mathbf{u}_f \right| \left(\mathbf{u}_g - \mathbf{u}_f \right)$$

- where (Wallis, 1969)

$$C_{f,i} = 0.005 \left(1 + 300 \frac{\delta}{D_h} \right)$$

Liquid Film Model
Energy Conservation

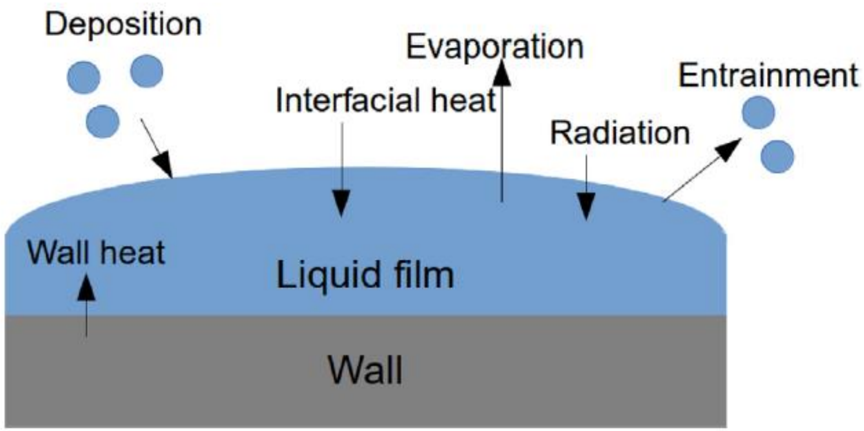

- Energy source terms for the liquid film

- Wall heat $$S_{h,q_w} = -k_l \left(\frac{\partial T}{\partial z} \right)_{z=0}$$
- Interfacial heat flux
$$S_{h,q_g} = -k_{geff} \left(\frac{\partial T}{\partial z} \right)_{z=\delta}$$
- Film evaporation
$$S_{h,vap} = S_{\delta,vap} h_{fg}$$
- drop deposition
$$S_{h,dep} = \dot{m}_{dep} h_d$$

Gas Core Modelling

- Two approaches are used:
  - Eulerian-Eulerian
  - Eulerian-Lagrangian

- In Eulerian-Lagrangian framework
  - the gas phase is treated as a continuum, described with the RANS equations
  - droplets are solved by Lagrangian Particle Tracking (LPT) approach, accounting for the mass, momentum and energy exchange with the gas field
- In Eulerian-Eulerian framework
  - both phases are treated as a continuum, described with the RANS equations

ROYAL INSTITUTE OF TECHNOLOGY

Turbulence Modelling in the Gas Core

- In Eulerian-Lagrangian framework
  - the turbulence of the continuous phase is modelled with the k-omega-SST approach
  - the effect of droplets on turbulence is included

- In Eulerian-Eulerian framework
  - each phase is treated as a continuum, described with the RANS equations

Eulerian-Lagrangian Approach

- The continuous vapor equations are as follows:

$$\frac{\partial \rho}{\partial t} + \nabla \cdot (\rho \mathbf{U}) = \Gamma_g$$

$$\frac{\partial (\rho \mathbf{U})}{\partial t} + \nabla \cdot (\rho \mathbf{U}\mathbf{U}) = -\nabla p + \nabla \overline{\overline{\boldsymbol{\tau}}} + \rho \mathbf{g} + \Gamma_g \mathbf{U}_{ff} + \mathbf{M}_d$$

$$\frac{\partial (\rho h)}{\partial t} + \nabla \cdot (\rho h \mathbf{U}) = -\nabla \mathbf{q}'' + \Gamma_g h_{ff} + q_d'''$$

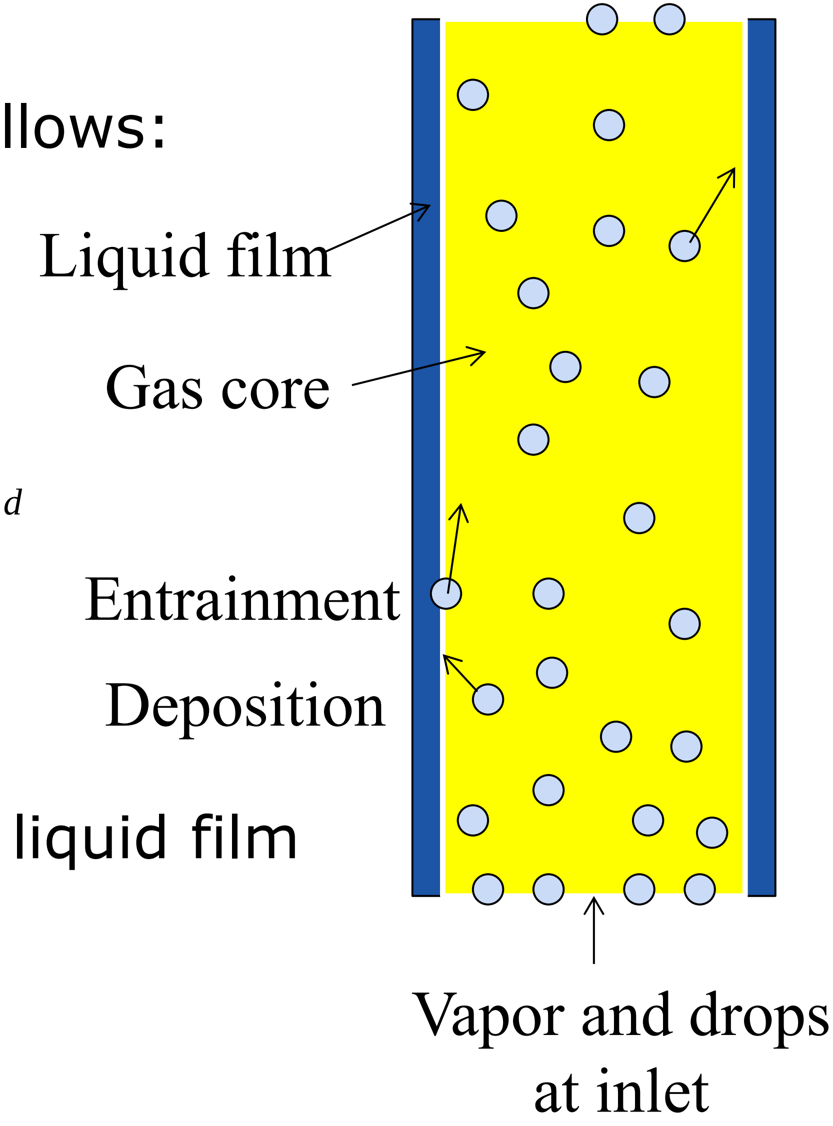

Γ_g mass source gained by the gas from liquid film

$\overline{\overline{\boldsymbol{\tau}}}$ effective stress

$\mathbf{M}_d$ Interfacial gas-droplets forces

Eulerian-Lagrangian Approach

- The droplet motion equations are as follows:

$$\frac{d\mathbf{x}_d}{dt} = \mathbf{v}_d$$

$$m_d \frac{d\mathbf{v}_d}{dt} = F = \mathbf{F}_D + \mathbf{F}_L + m_d \mathbf{g}$$

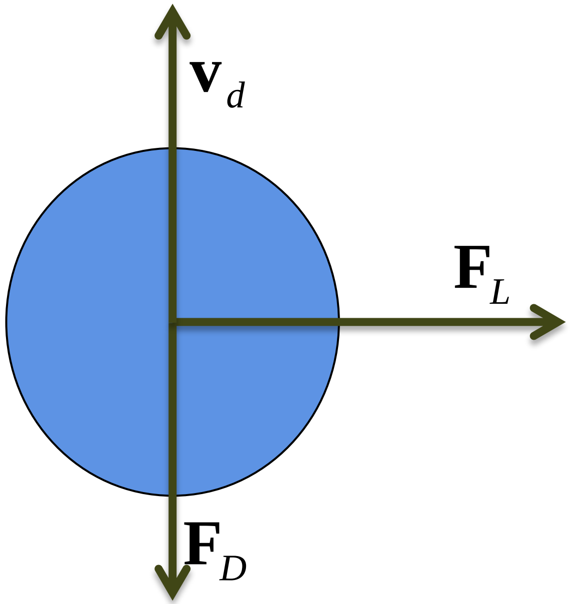

m_d	mass of a droplet
$\mathbf{F}$	total force
$\mathbf{F}_L$	lift force

Lagrangian Particle Tracking

GOAL: To model drop deposition in complex geometries and to take into account spacer effects

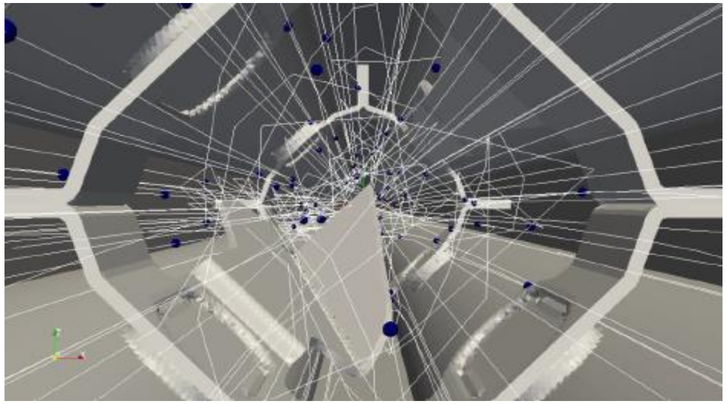

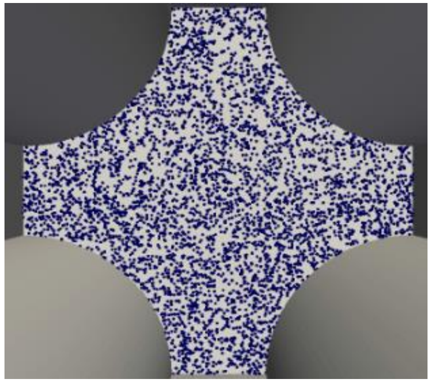

Inserting drops at inlet and at film surface (entrainment)

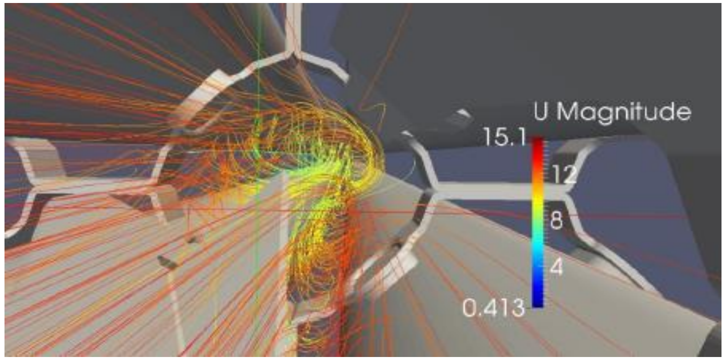

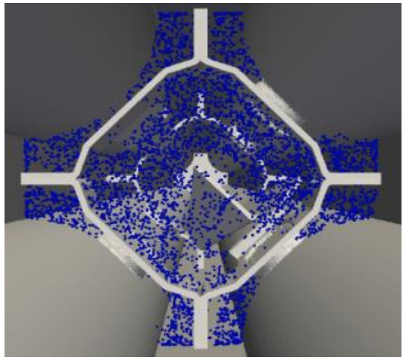

Eulerian-Eulerian Approach

- The droplet motion equations are as follows:

$$\frac{\partial \alpha_k \rho_k}{\partial t} + \nabla \cdot (\alpha_k \rho_k \mathbf{U}_k) = \Gamma_k$$

$$\frac{\partial (\alpha_k \rho_k \mathbf{U}_k)}{\partial t} + \nabla \cdot (\alpha_k \rho_k \mathbf{U}_k \mathbf{U}_k) = -\alpha_k \nabla p + \nabla \left(\alpha_k \overline{\overline{\boldsymbol{\tau}}}\right) + \alpha_k \rho_k \mathbf{g} + \Gamma_k \mathbf{U}_{ki} + \mathbf{M}_{ki}$$

$$\frac{\partial (\alpha_k \rho_k h_k)}{\partial t} + \nabla \cdot (\alpha_k \rho_k h_k \mathbf{U}_k) = -\nabla (\alpha_k \mathbf{q}'') + \Gamma_k h_{ki} + q'''_{ki}$$

Γ_k mass source for phase k

$\mathbf{M}_{ki}$ interfacial momentum transfer

$\mathbf{U}_{ki}$ phase-k velocity at the interface

Coupling of the Gas Core with the Liquid Film (for Mass Transfer)

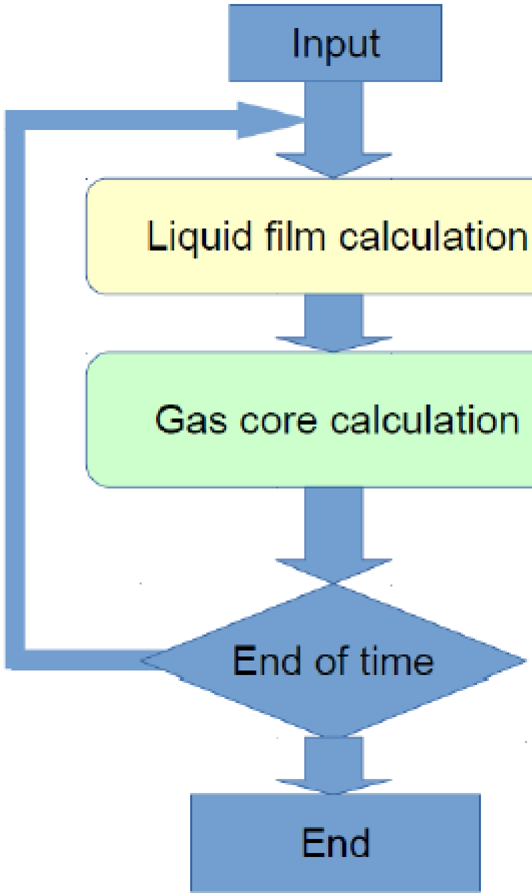

- The liquid film calculations give source terms for the gas flow calculations
- Gas core calculations prepare sources for liquid film calculations in the next time step
- Transient solution scheme is adopted

ROYAL INSTITUTE OF TECHNOLOGY

Dryout Prediction Approach

Nuclear Reactor Technology KTH

THREE FIELDS

- **LIQUID FILM** – 2D Eulerian ⟺ **Film Thickness = δ_{cr} ⇕ Dryout**
- **VAPOUR/GAS** – 3D Eulerian
- **DROPS** -
  - Lagrangian
  - Eulerian

3D CMFD
k-ε Turbulence Model
Transient & Steady State

IAC transport equations

HEAT TRANSFER

- **Wall-droplet direct heat transfer**
- **Radiation heat transfer**
- **Wall temperature function**

Onset-of-Dryout Criterion

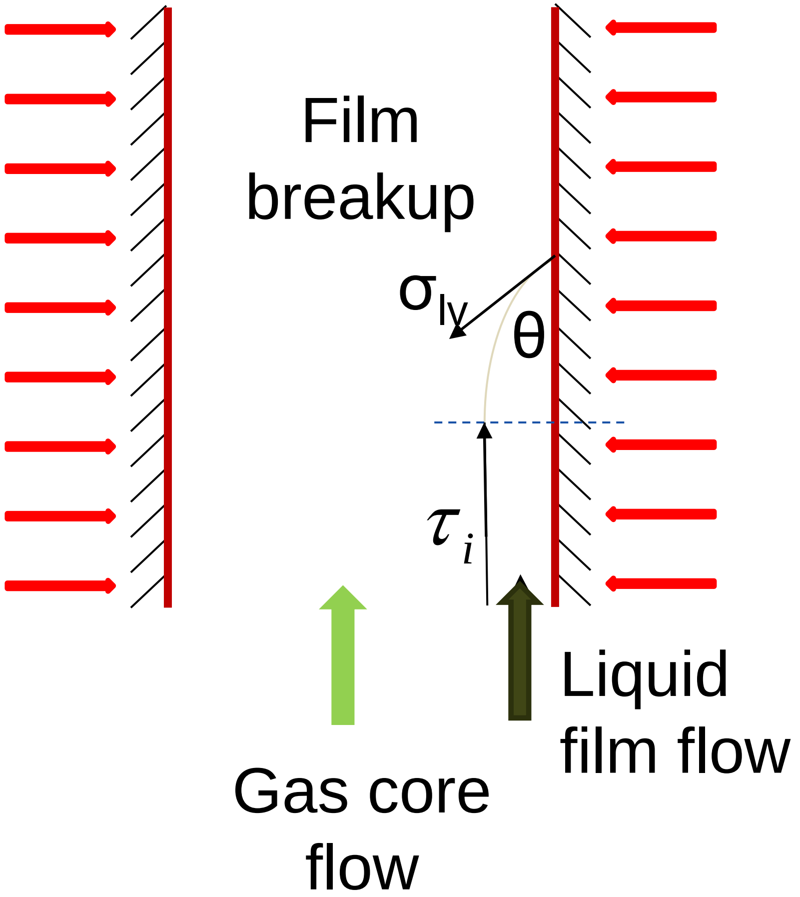

- Liquid film is assumed to breakup when the film thickness is less than the critical heat thickness

- Two models for the critical film thickness are considered:
  - Chun et al. (2003):

$$\delta_c = \left(\frac{q''}{h_{fg} G_{ff}} \right)^{0.35} \frac{\upsilon_{fg} \mu_f^2}{\sigma} \times 10^{8.8\left(\frac{\mu_g}{\mu_f}\right)^{0.617}}$$

  - Anglart (2011, 2013, 2015) – mechanistic model of the minimum wetting rate in a closed channel

Modelling of Post-Dryout Heat Transfer

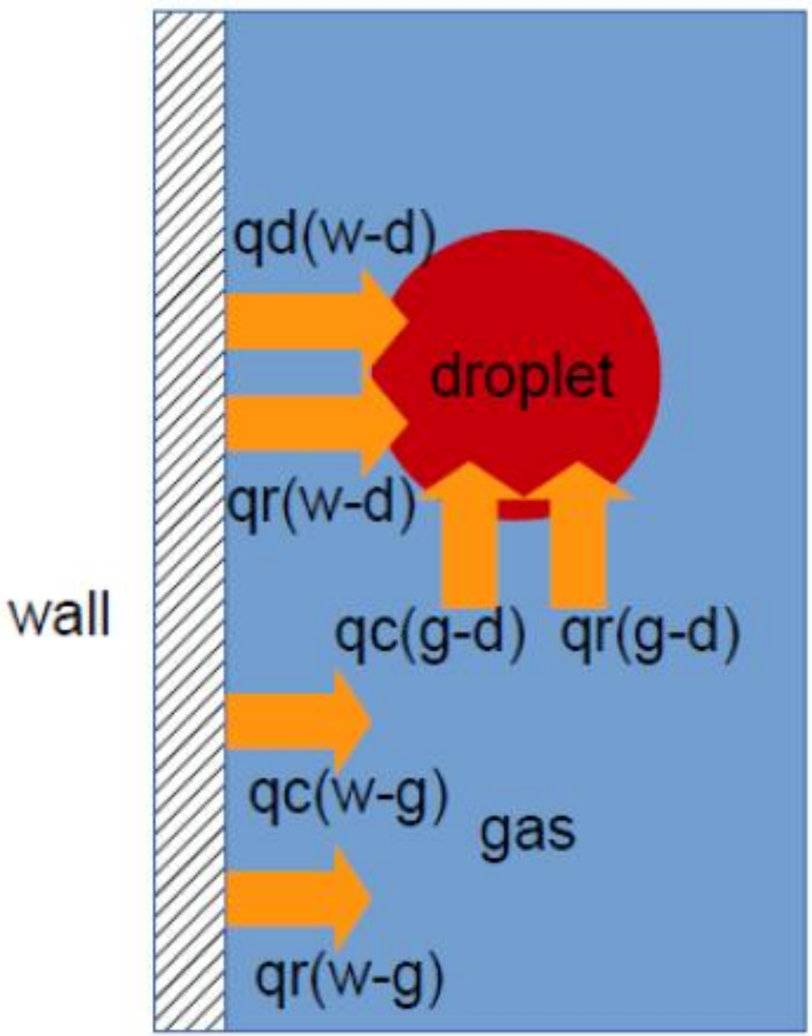

- The following transfer mechanisms are included
  - wall-gas heat transfer, qc(w-g)
  - gas-droplets interfacial heat transfer qc(g-d)
  - wall-droplet direct contact heat transfer qd(w-d)
  - thermal radiation between the wall, the gas and the droplets, qr(w-g), qr(w-d), qr(g-d)

Experimental Data used in Validation of the Model

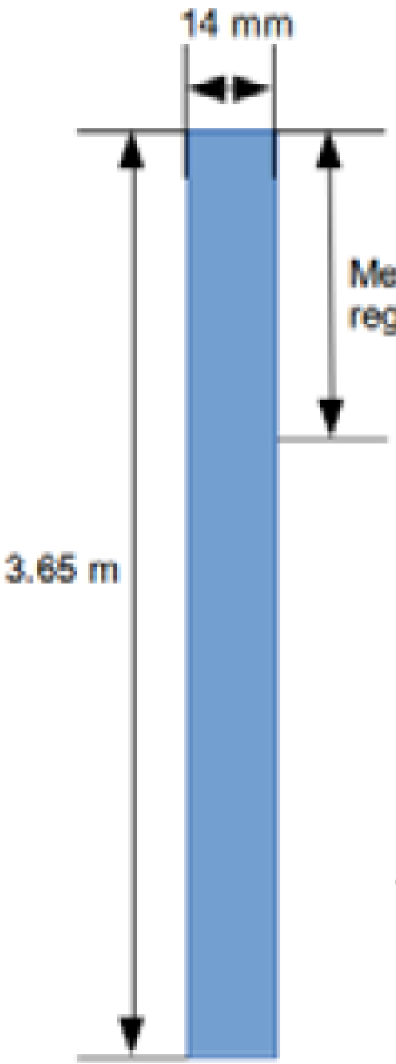

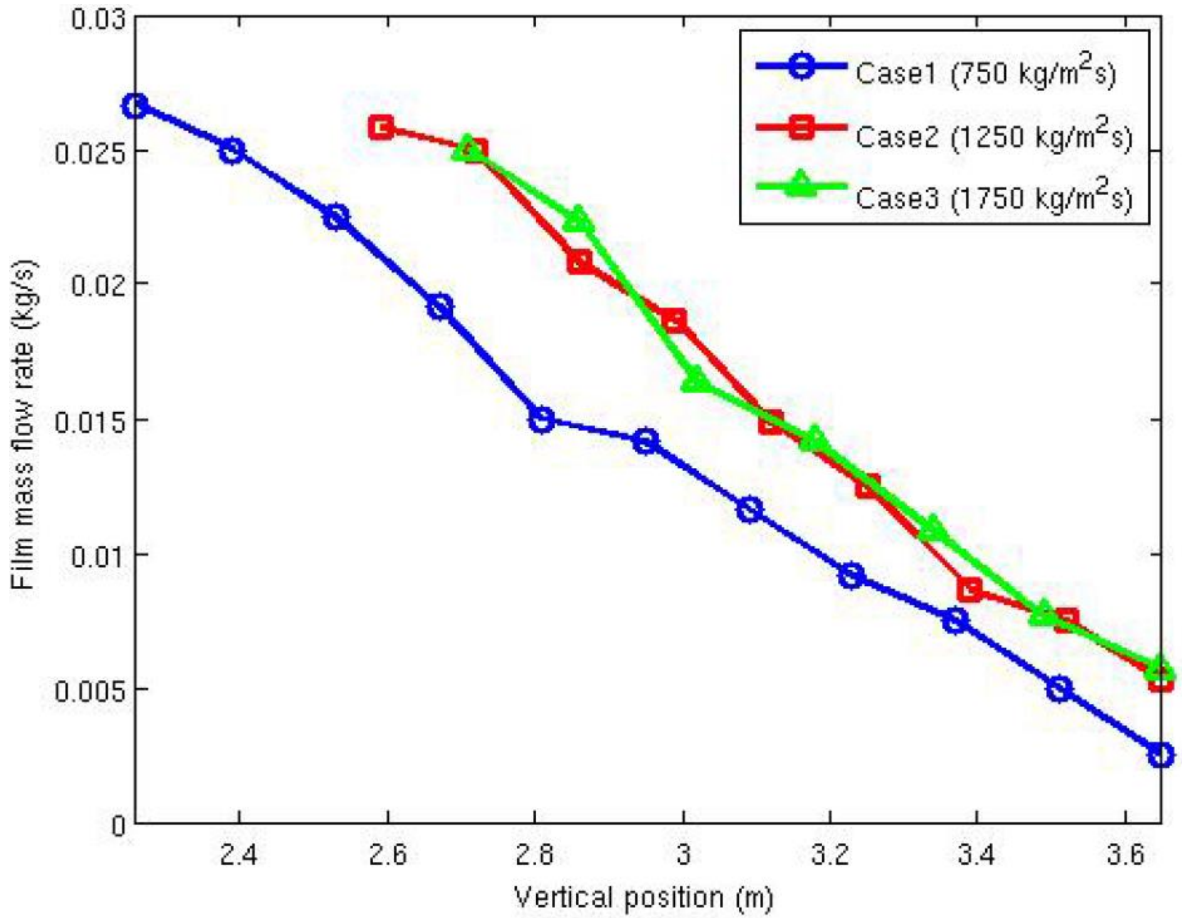

- Liquid film flow rate was measured for annular flow in a pipe of 14 mm ID at 7 MPa and mass fluxes 750, 1250 and 1750 kg/m^2s (Adamsson and Anglart, NED, 2006)

Computational Geometry and Grid

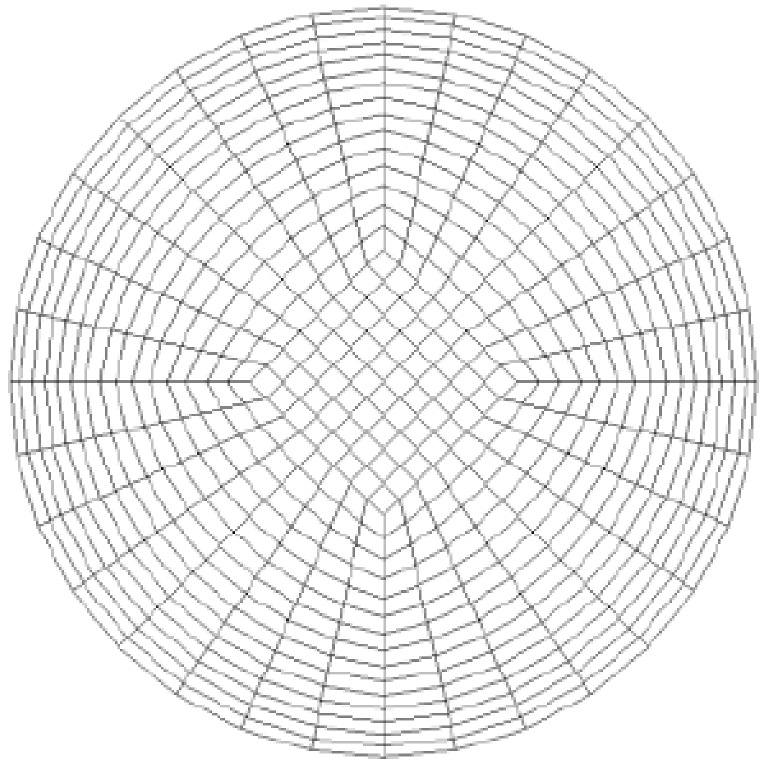

- Multiblock hexahedral mesh
- 270 K mesh selected after mesh sensitivity study
- 54.4 K mesh used for Eulerian-Lagrangian calculations

Liquid Film Flow Rate for Case 1 (750 kg/m²s)

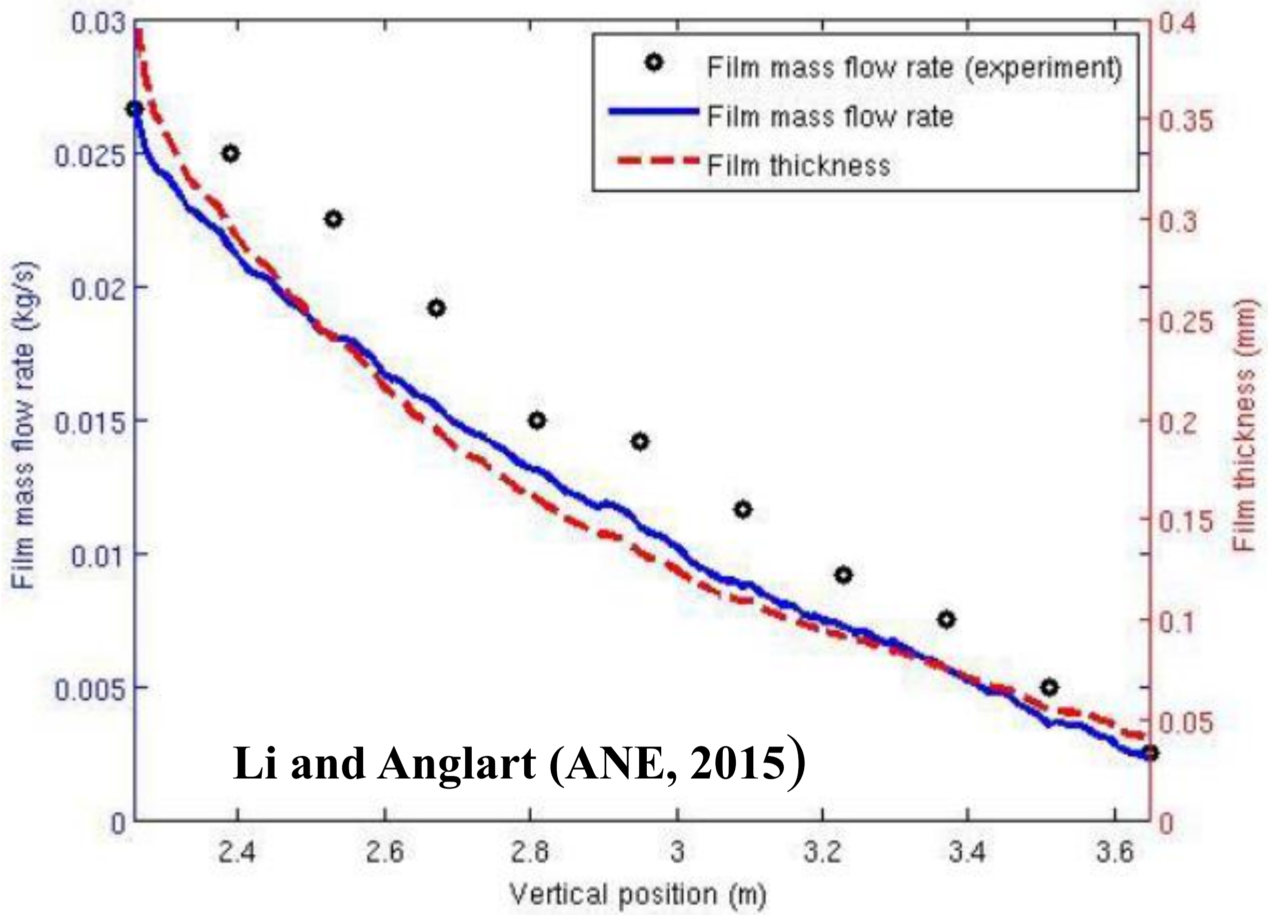

- Eulerian-Lagrangian approach is used
- Only annular flow region of the pipe is modelled
- Liquid film flow rate is underpredicted due to entrance effect, where entrainment rate is too high
- Improved accuracy close to the outlet

Liquid Film Flow Rate for Case 2 (1250 kg/m²s)

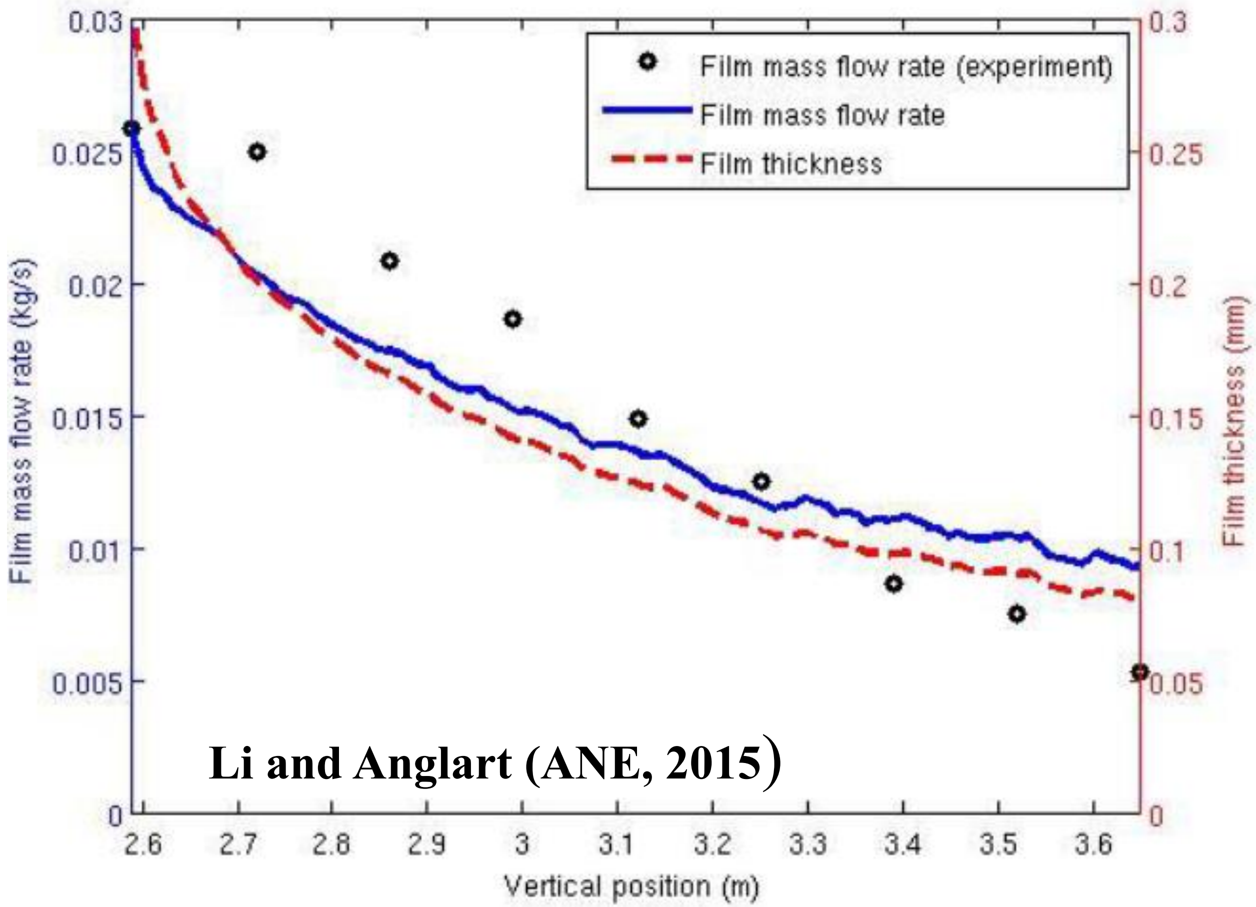

- Eulerian-Lagrangian approach is used
- Only annular flow region of the pipe is modelled
- Liquid film slightly over-predicted towards the channel outlet

Predicted and Measured Mass Transfer Rates

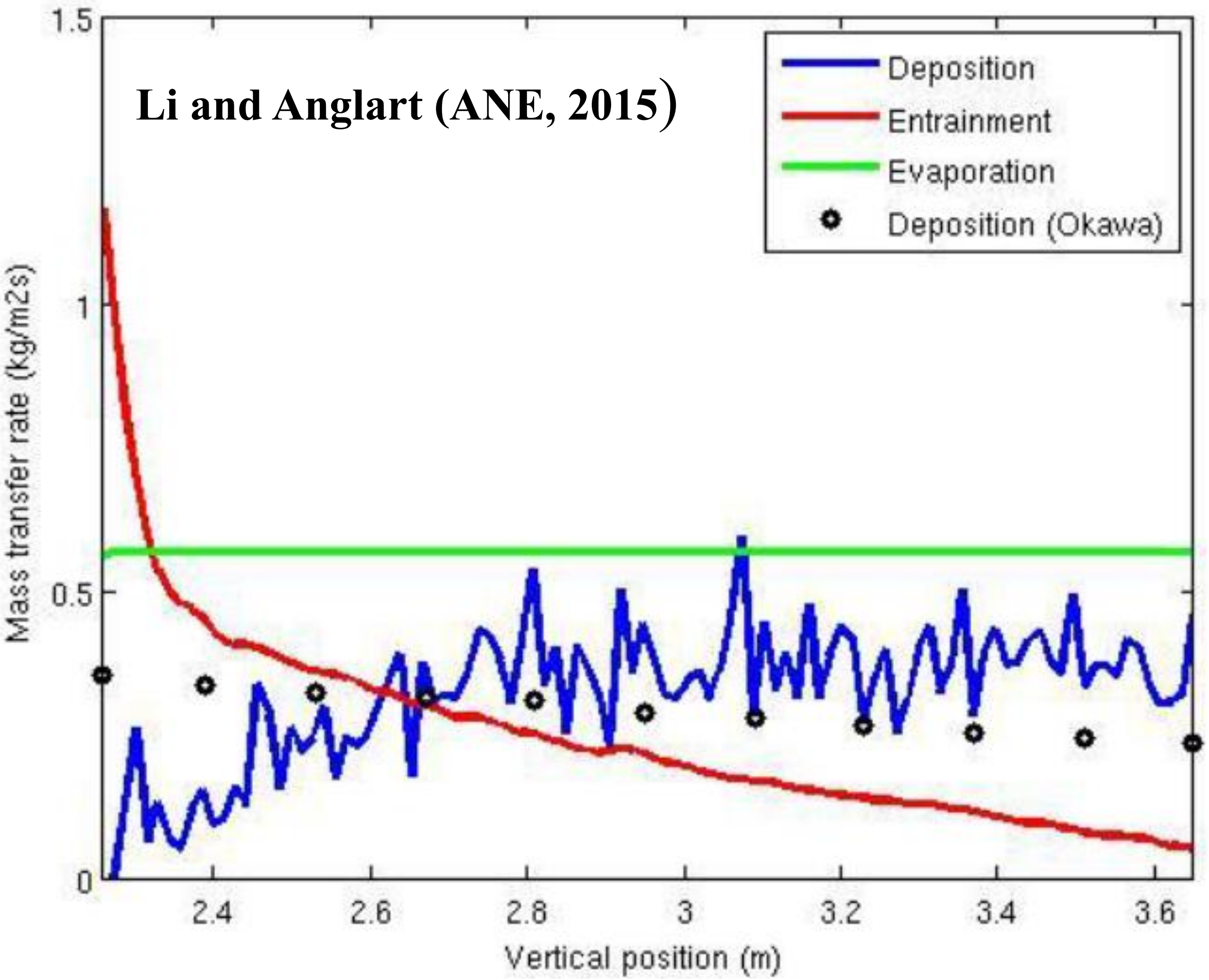

- Deposition rate obtained in Eulerian-Lagrangian approach is shown
- The predictions agree fairly well with the correlation based on experimental data (Okawa)
- Stron over-prediction of the entrainment rate at the inlet

Experimental Data used in Validation of the Dryout Model

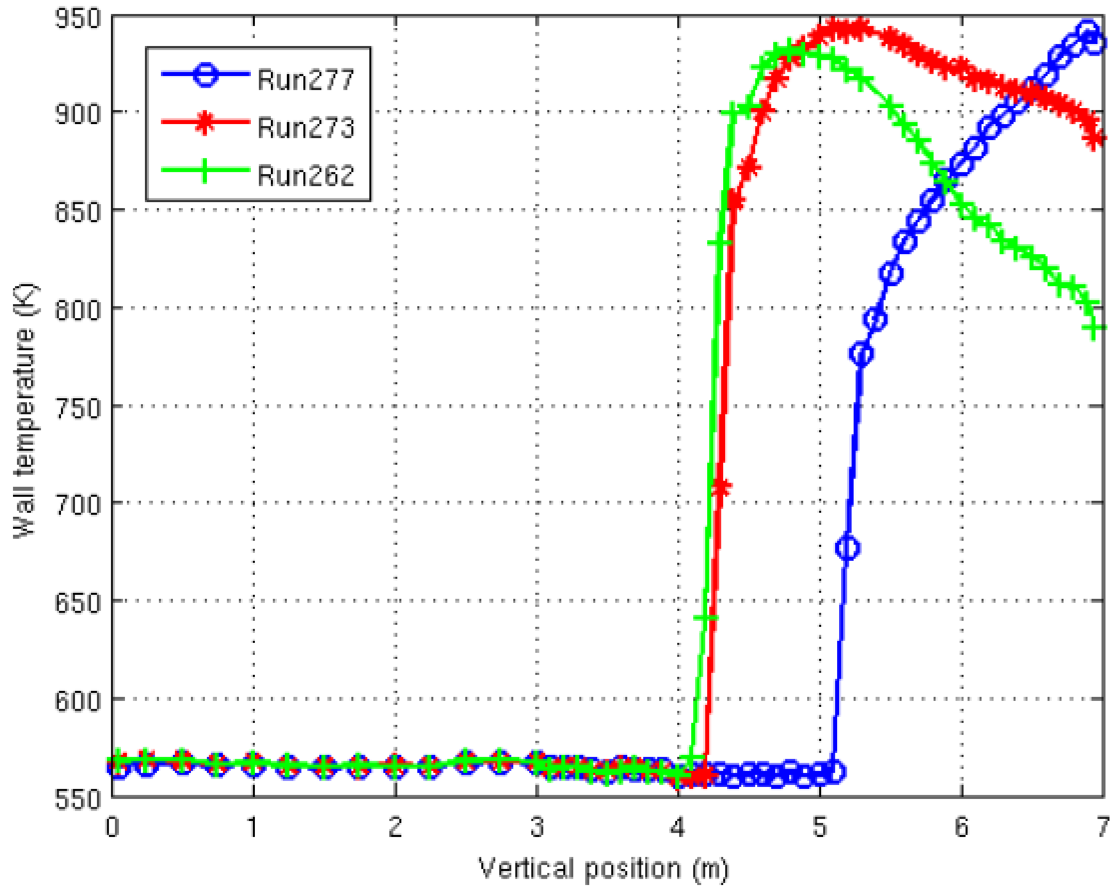

- Three experimental cases: uniformly heated tube with 14 mm ID, pressure 7 MPa, mass flux 500, 1000 and 2000 kg/m2s (Becker et al., 1983)

Comparison of Predictions to Experimental Data

- Run 277 (G = 500 kg/m²s)
- Run 273 (G = 1000 kg/m²s)
- Run 262 (G = 2000 kg/m²s)

Li and Anglart (2015)

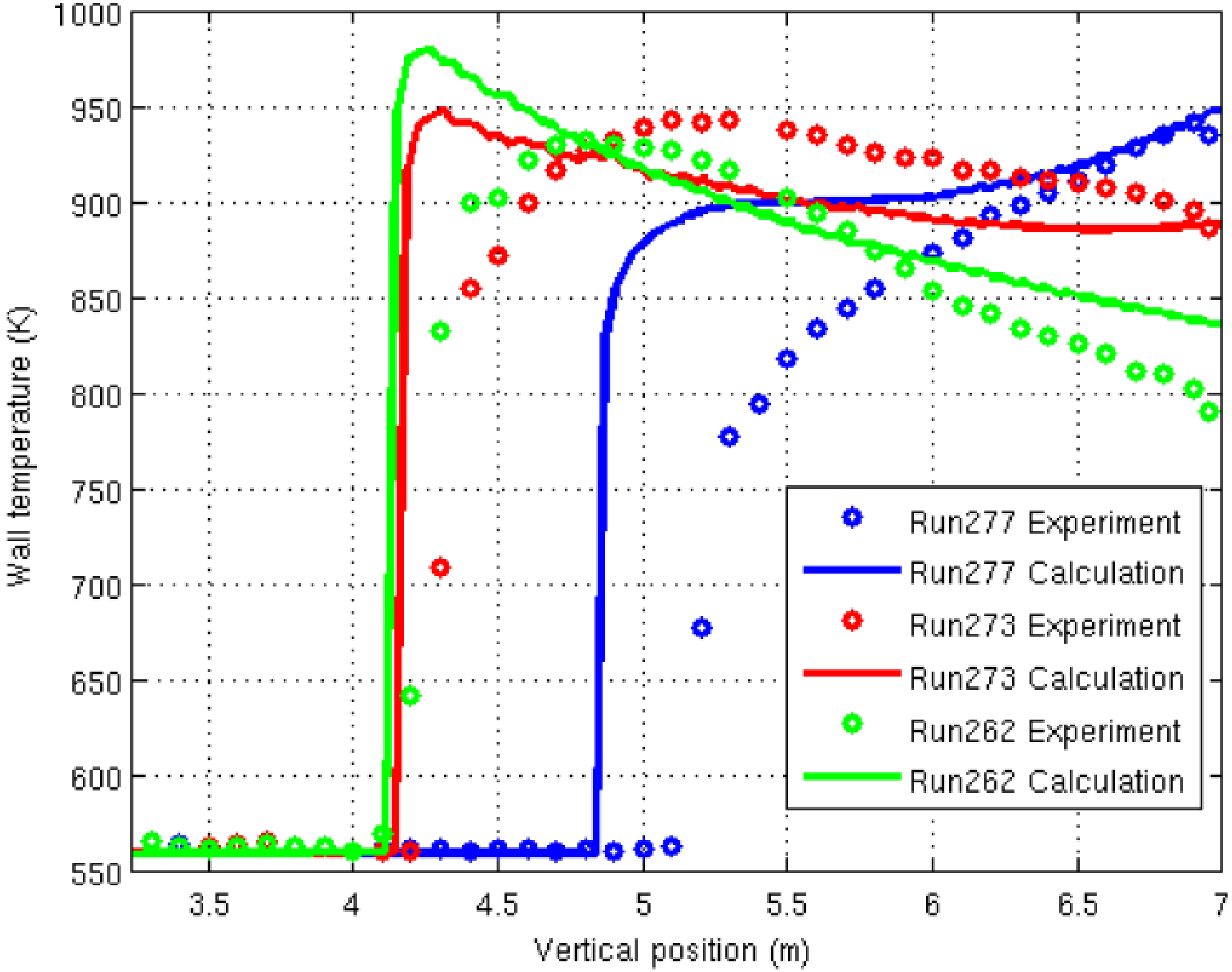

Sensitivity Study of Dryout Location to Entrainment/Deposition

- Run 262 (G = 2000 kg/m^{2}s)

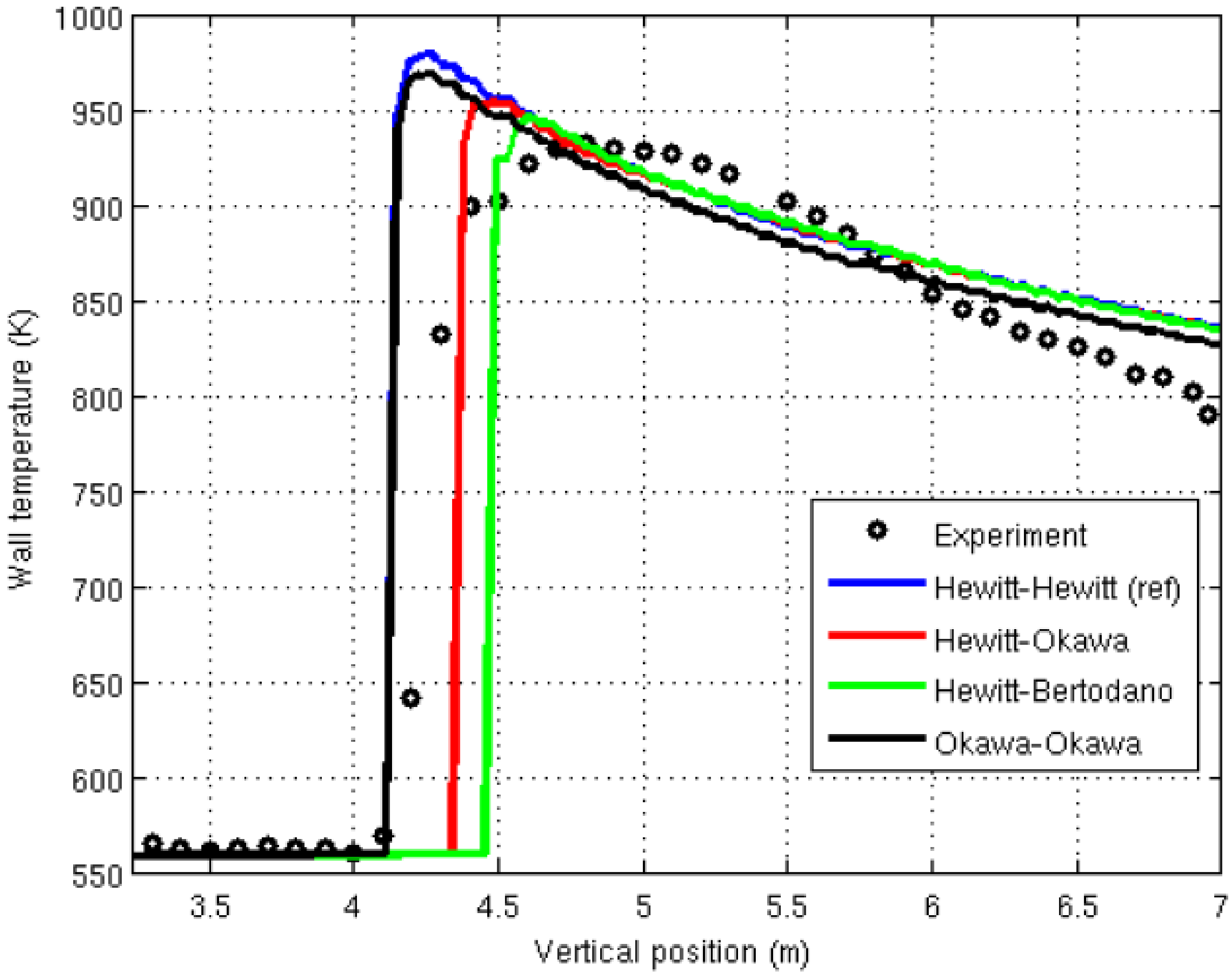

Li and Anglart (2015)

Application of the Models to Rod Bundle Geometry

- Conditions corresponding to BFBT experiments:
  - p: 70 bar
  - inlet drop velocity: 10 m/s
  - inl. drop vol. frac.: 6%
  - inl. liq. film thickn.: 0.1 mm
  - inl. liq. film vel. : 4.5 m/s
  - heat flux rods 1,2,4: $1 MW/m_2$
  - heat flux rod 3: $1.2\ MW/m^2$

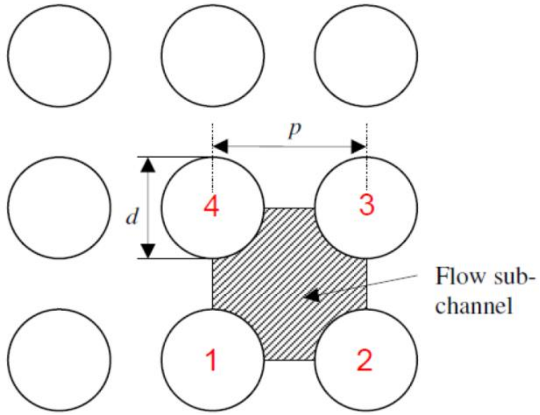

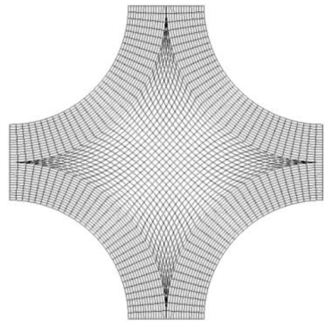

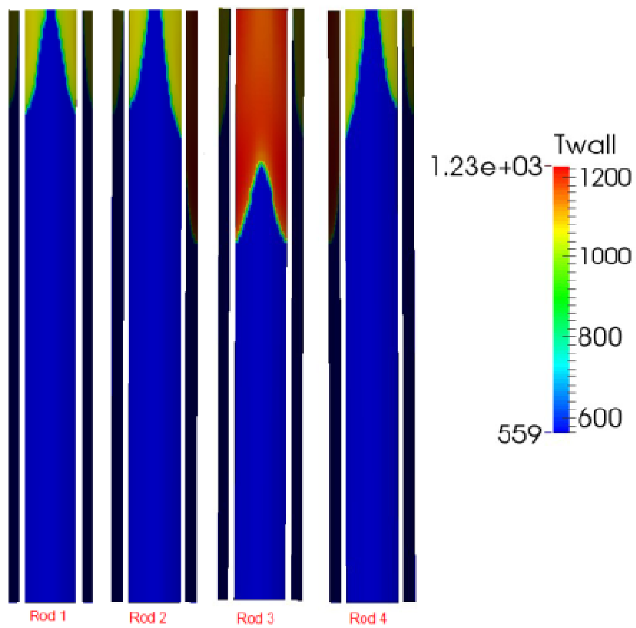

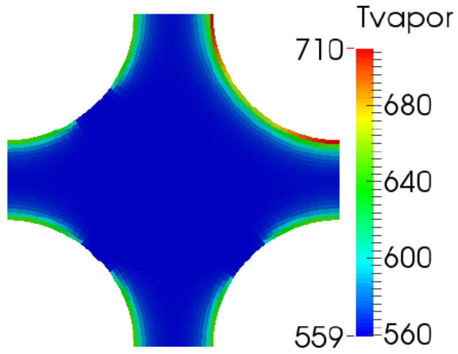

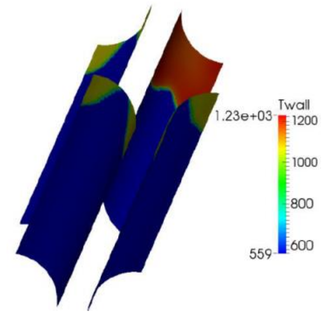

Li and Anglart (2015)

Conclusions

- Significant progress in numerical methods (CFD) has been achieved during recent 30 years
- Better understanding of the governing phenomena
- Current approach:
  - for turbulent mixing: carefully validated LES
  - for DNB: modelling of small scales (nucleation sites, microlayer) and simulation of larger scales (bubbles, macrolayer, bulk)
  - for dryout: modelling of interfacial mass, momentum and energy transfer in annular flow, including liquid film breakup; simulation of gas core flow and 2D liquid film
- What is missing?
  - detailed experimental data allowing development and validation of sub-models and closure laws between scales and fields

Thank You!